Topographical dynamics based on global and UAV-SfM derived DEM products: A case study of transboundary Teesta River, Bangladesh

B. M. Refat Faisal[1, 2]

Email: refatfaisal@ees.hokudai.ac.jp

Yuichi S. Hayakawa[3]

Email: hayakawa@eis.hokudai.ac.jp

(Institutional addresses)

[1] Graduate School of Environmental Science, Hokkaido University, Sapporo, Hokkaido 060-0810, Japan.

[2] Bangladesh Space Research and Remote Sensing Organization (SPARRSO), Agargaon, Sher-e-Bangla Nagar, Dhaka-1207, Bangladesh.

[3] Faculty of Environmental Earth Science, Hokkaido University, Sapporo, Hokkaido 060-0810, Japan.

Topographical dynamics based on global and UAV-SfM derived DEM products: A case study of transboundary Teesta River, Bangladesh

Abstract

Topographical changes in riverine floodplains need to be measured for assessing geomorphological dynamics and protecting floodplain areas, although topographic evaluation in disaster-prone floodplain in South Asia has been limited due to the lack of multitemporal, high-definition digital elevation models (DEMs) derived from modern techniques including airborne laser scanning, structure-from-motion (SfM) photogrammetry accompanied with Unmanned Aerial Vehicle (UAV, often referred as drone), and field-based mapping approaches. Here we conducted a preliminary study at two locations of Teesta River (Brahmaputra's tributary) in Bangladesh using the UAV-SfM techniques and generated high-resolution DEMs. The selected locations represent dynamic changes of sediment and water on the floodplain over the years, and the UAV-SfM approach can be an effective method for monitoring those changes, but an archive of the past data has been unavailable. Here we evaluated the topographic changes by comparing the UAV-SfM-derived DEMs of 2022 with global DEM products (NASADEM of 1999), which are often the only available choice of DEMs in this river floodplain. The elevation differences of these two sets of DEMs were in the range of −5.23 to −84.66 m, and volumetric changes of −4.11±0.15 to −86.25±0.20 million m^3, likely dominated by erosional processes towards the left side bank where the elevation errors are supposed to be several meters for UAV-DEM and ca. 5-12 m for NASADEM. Although it is not easy to accurately evaluate the absolute values of the changes, these changes may be associated with the upper basin's morphodynamics. The considerable changes in topography indicate the importance of continuous terrain evaluation in disaster-prone floodplains.

Keywords: Unmanned aerial vehicle (UAV); Structure-from-motion (SfM); NASADEM; DEM of difference (DoD), Cross-sectional profiles; Volumetric change estimate; Geomorphology.

1. Introduction

In fluvial geomorphology, river topography measurement is a significant concern and a basic descriptor for understanding the geomorphic processes (Woodget et al. 2014; Özcan and Özcan 2021). The analysis of spatiotemporal modifications of the river, which are suddenly changing the flow pattern and hydro-geomorphology due to natural and anthropogenic factors, requires better hazard assessment since these processes can result in flood phenomena and suffering to human society (Rinaldi et al. 2017; Fanta-Jende et al. 2020). In this regard, the river topographic model plays a critical role in investigating a range of the earth's surface processes and detailed monitoring of the fluvial environment (Watson et al. 2019; Salandra et al. 2022). For topographic studies, freely accessible global digital elevation model (DEM) products such as National Aeronautics and Space Administration DEM (NASADEM, released in 2020), ALOS Global Digital Surface Model (AW3D30, released in 2020), TerraSAR-X add-on for Digital Elevation Measurement (TanDEM-X, released in 2018), Multi-Error-Removed Improved-Terrain (MERIT, released in 2017), Advanced Spaceborne Thermal Emission and Reflection satellite (ASTER, released in 2006), and Shuttle Radar Topography Mission (SRTM, released in 2003) are often used in the absence of finer resolution data which is limited for multitemporal assessment (Watson et al. 2019; Uuemaa et al. 2020). Among the existing freely available global DEM data sets, the NASADEM, reprocessed from the STRM-1999 measurement offer near-global land surface coverage at 30 m spatial resolution has been considered here as baseline topography because of its recent improvements and accuracy (NASA JPL 2020; Uuemaa et al. 2020; Tran et al. 2023). The orbital nature of satellites hampered the revisit frequency (i.e., low temporal resolution) to the same location, so it is not easy to track dynamically changing rivers (Rhee et al. 2018).

The recent advents in Unmanned Aerial Vehicles (UAVs) or Dynamic Remotely Operated Navigation Equipment (DRONE) are advantageous over satellite and piloted aircraft in data acquisition which is widely used in monitoring dynamic changes in river morphology

(Van Iersel et al. 2016; Rusnák et al. 2018; Cai et al. 2022), natural hazards management (Giordan et al. 2018), and water resource management (Acharya et al. 2021). The UAV (DRONE) is defined as an unmanned aerial system that can have an autonomous flight with or without an engine, be remotely controlled, and be able to collect data (Giordan et al. 2020; Acharya et al. 2021; Oguchi et al. 2022). The high-resolution DEMs generated from UAVs following the structure-from-motion (SfM) multi-view stereo photogrammetry (SfM-MVS) workflow are becoming increasingly common for assessing earth surface processes (Smith et al. 2015). Several studies, for example, Annis et al. (2020), Avand et al. (2022), Oguchi et al. (2022), and Salandra et al. (2022), demonstrated the importance of high-resolution DEMs for more accurate geomorphological and topographical analysis. The advances in survey equipment (i.e., UAVs, LiDAR) and data processing software (i.e., Agisoft Metashape) enable the production of rapid and accurate high-resolution topographic data (i.e., DEMs), over the decades in river environments (Picco et al. 2023). The characterization of hydro-geomorphological features, channel planform changes, and sediment dynamics (erosion and deposition processes) can be performed using high-resolution topographic analysis, which can significantly improve our understanding of fluvial regimes (Salandra et al. 2022). The advanced remote sensing techniques (i.e., LiDAR-light detection and ranging, UAV-SfM) are encouragingly used in East and South Asian countries like China, India, Bhutan, Nepal, and Pakistan for fluvial-geomorphic research (Faisal and Hayakawa 2022). In contrast, the UAV-based approaches in fluvial geomorphological and topographical studies are still scarce or have not started in the context of the Ganges-Brahmaputra-Meghna (GBM) river system in downstream Bangladesh which is highly influenced by the upper basin's morphodynamics, hydrology, sediment flux, and anthropogenic stressors (Faisal and Hayakawa 2022, 2023).

The recent advancement of fluvial research mentioned by Oguchi et al. (2022) and the geomorphic research gaps in large South Asian GBM Rivers by Faisal and Hayakawa (2022,

2023) necessitates the UAV-based topographic survey to assess the geomorphic features at Brahmaputra's river system that changes dramatically. In Bangladesh, several scholars have employed multi-temporal satellite imageries to investigate the Teesta River (Brahmaputra's tributary), focusing on channel dynamics (Khan and Hossain 2001; Khan et al. 2015; Ashrafi et al. 2016; Akhter et al. 2019), channel bar evolution (Ghosh 2014; Khan and Islam 2015), and water flow patterns (Mullick et al. 2010; Mondal and Islam 2017). Besides, several studies about morphological dynamics also exist in the upper part of the transboundary Teesta River in India, such as Mandal and Chakrabarty (2016), Goyal and Goswami (2018), and Lukram and Tandon (2022). Furthermore, the evidence of anthropogenic stressors (i.e., dams, channelization, barrages, channel diversions, and hydroelectric projects) on morphological characteristics and sediment dynamics along the Himalayan basin is also mentioned in earlier studies (Kale 2002; Zarfl et al. 2015; Goyal and Goswami 2018; Higgins et al. 2018; Best 2019; Palash et al. 2023; Raff et al. 2023). Also, in the future, a boom in hydropower dam construction activity in Asia, mainly in China, India, and Nepal is reported (Zarfl et al. 2015), which can significantly affect the sediment supply to the downstream delta (Darby et al. 2015; Dunn et al. 2018; Higgins et al. 2018; Raff et al. 2023).

Unfortunately, little or no attention has been paid to the past literature on topographic change studies due to the unavailability of multitemporal topographic data in the Teesta River that may have significant implications for understanding the sedimentation pattern and river floodplain management in disaster-prone South Asian region. The present area of interest mostly relies on freely accessible terrain data sources. Hence, the topographic survey for introducing high-resolution terrain data has become necessary for investigating this region's topography and associated geomorphic dynamics. Therefore, the present work focuses on utilizing UAV imageries and newly available NASADEM to assess the river's topographical dynamics as well as to show the potential applicability of advanced remote sensing techniques

(UAV-SfM) in developing areas of South Asia, Bangladesh along the Brahmaputra's tributary (Teesta River).

The combination of advanced UAV-SfM techniques and satellite remote sensing embedded with field-based approaches may be helpful for topographic change studies, as the multitemporal DEMs were unavailable for the present area of interest. Recently, several studies have been conducted in different parts of the world deriving the topographical and morphological dynamics comparing the UAV-DEMs to the global DEM products, such as Hsieh et al. (2016) (Taiwan), Watson et al. (2019) (Nepal), Tang et al. (2019) (China), and Parizi et al. (2022) (Iran). Although the UAV survey will cover small area compared to the enormity of the Teesta River, this study definitely fills the knowledge gaps of the previous studies. The present study is attempted as a novel case study in deriving UAV-SfM-based high-resolution topography (UAV-DEM) and later compared with the available global DEMs (NASADEM) to evaluate the topographical dynamics and fluvial-geomorphic processes in South-Asian context focusing at Teesta River, Bangladesh. Hence, we assume that the dynamics of topographic and volumetric changes (erosion and deposition) of a flood-vulnerable transboundary Teesta River in the Bangladesh floodplain can be quantified from the calculation of the difference between two subsequent DEMs (DEM of Difference: DoD) (UAV-DEM 2022 and NASADEM 1999) (Wheaton et al. 2010; Picco et al. 2023). Therefore, this article aimed to a) assess the topography and geomorphological features focusing on changes in elevation, volumetric estimates, and river cross-sectional profiles at disaster-prone Teesta River, and b) introduce UAV-SfM techniques for high-resolution data acquisition in the lowland river environment as a baseline topographic survey. The study's outcomes will help to understand the topographical dynamics and fluvial-sedimentation processes and the potential applicability of UAV-SfM techniques, which can play a crucial role in taking adaptive strategies for river floodplain management and reducing people's suffering from repeated sediment disasters.

2. Materials and methods

2.1 Study area and UAV mission planning

This study has been conducted in the transboundary Teesta River that flows through the highlands in Sikkim, the hills of West Bengal, and the floodplains of West Bengal (India) and Bangladesh (Figure 1). This river has a length of 414 km, drains an area of around 12,159 km^2, and traverses two different countries "India" (83%) and "Bangladesh" (17%) (Alford 1992). This transboundary river's flow regime has been affected mainly due to large-scale damming, causing devastating floods and bank erosion in downstream Bangladesh (Mirchandani 2016). For instance, severe flooding of the upper Teesta River valley originated from the South Lhonak Lake's GLOFs (Glacial Lake Outburst Flood) on 4th October 2023, affected tens of kilometers downstream, resulting in loss of human life (14 people) with severe damage to the buildings, highways, and collapsing of Chungthang dam (Sattar 2023; Chauhan 2023). In Bangladesh, the Teesta River traverses (170 km) through the extreme northern part of Bangladesh (Nilphamari, Lalmonirhat, Kurigram, Rangpur, and Gaibandha district) and is crucial for almost 10 million people in this region (BBS 2016; Islam 2016). The Teesta floodplain covers around 14% of the country's total cultivated land and is one the largest geomorphic units of Bangladesh (Akhter et al. 2019). It plays a crucial role in flushing silt and sediment deposited during the dry season, the region's lifeline for irrigation, agriculture, farming, fishing, and navigation (Prasai and Surie 2013). The sediments are mainly recent floodplain deposits comprising of clay, silt, fine, and medium-grain sand (Islam et al. 2014). The study area falls in a sub-tropical monsoon (June to September), mostly dry climatic region (pre-monsoon and post-monsoon), where mean annual rainfall is more than 1900 mm (decadal 2010-2019 average of 2408 mm) with mean temperature of 35°c and 15°c in the summer and winter seasons, respectively (Rahman et al. 2011; Akhter et al. 2019; Faisal and Hayakawa 2023). The annual average discharge of Teesta River ranges from (280−470 m^3/s) over the 2011−2022 period, where extreme low-flow conditions (<50 m^3/s) (Figure 2) during the dry season are likely to occur more frequently after India implemented the Gazoldoba barrage in 1993 (Higano and Islam 2002; Ghosh 2014; Islam 2016; Pangare et al. 2021).

Unfortunately, the exclusive control of Teesta's upstream water in the dry season at Gozoldoba (India) makes the Teesta barrage (operation started in 1990) useless and fails the irrigation project in northern Bangladesh (Khan 2001; Mondal and Islam 2017; Goyal and Goswami 2018). Furthermore, the sudden release of excessive water in the rainy season causes flood and bank erosion, leading to severe suffering for the people in Bangladesh (Higano and Islam 2002). Given the large area of the Teesta River in Bangladesh (>2071 km^2), this study selects two cross-sections considering the minimal UAV survey coverage, assumed to be representative of the river's topographical and morphological features investigation focusing on dynamics changes of sediment and water on the floodplain over the years (Mondal and Islam 2017; Akhter et al. 2019). The selected two cross-sections (CS-1 and CS-2) were relatively upstream and downstream from the location of the Teesta barrage (Figure 1C), which is one of the anthropogenic interventions along the main river channel.

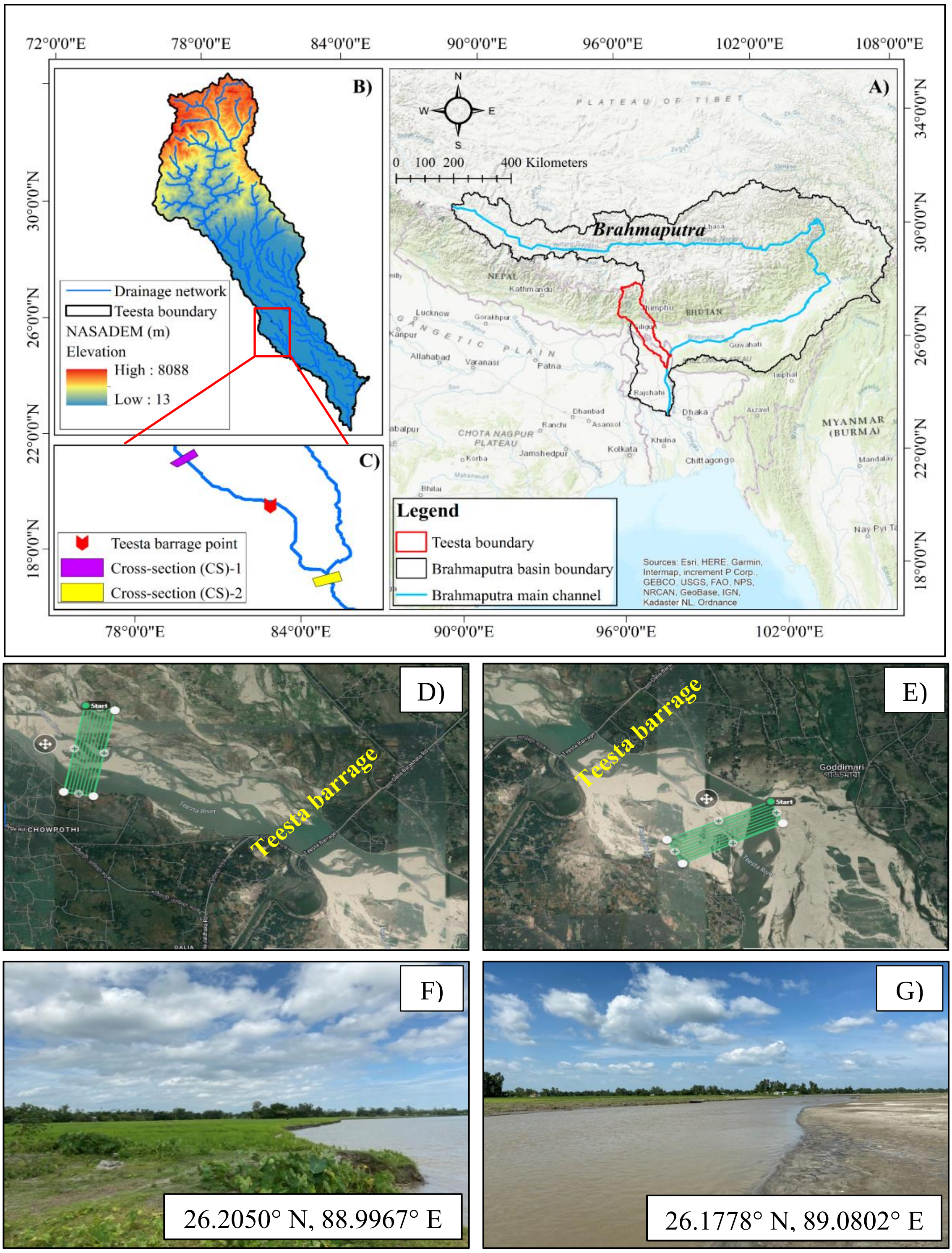

Figure 1: A) Overview of study sites in Teesta River (Brahmaputra's tributary) showing the transboundary flow regime, B) elevation map with drainage channel, C) enlarged view of selected cross-sections, D-E) example of mission plan in DroneDeploy for CS-1 and CS-2, and F-G) field picture showing the erosion along the bank at CS-1 and CS-2 taken in Aug 2022.

The UAV survey (drone flight) was planned in DroneDeploy, where Google Earth Pro was used to select the mission coordinates. The UAV used for the image recording is the DJI Mavic 2 Pro (equipped with a 20-megapixel, 1-inch RGB CMOS sensor and 35 mm f 2.8 lens with a 77° field of view), adjusted the altitude in Height Above Ellipsoid (HAE) to elevation using EGM96 (Earth Gravitational Model 1996) geoid model. The UAV automatically captured imagery, and each image was georeferenced with 3D coordinates from the UAV's global navigation satellite system (GNSS) receiver. Multiple flights with more than 75% front overlaps and 60% side overlaps were ensured to reduce the dome effect and uncertainty in elevation measurement (James and Robson 2012; Hayakawa and Obanawa 2020). With this flight plan (Table 1), 775 and 1,050 photos were collected from CS-1 and CS-2, respectively (Figure 1D-E).

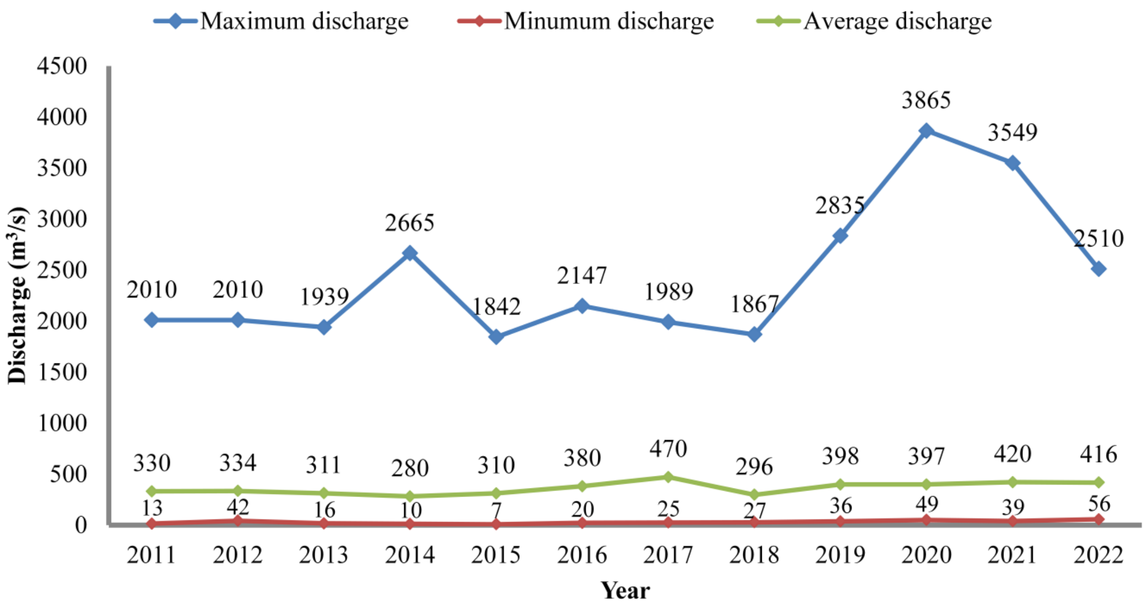

Figure 2: Yearly discharge experienced by study reach measured at Dalia (Teesta barrage) gauging station from (2011-2022) (Data source: Hydrology directorate, BWDB).

2.2 UAV and NASADEM data processing

The collected UAV imageries were processed using SfM-MVS photogrammetry software, Agisoft Metashape Professional (version 1.8.1 Build 13915, 64-bit), which can produce accurate DEMs from suitable photographs and are used for geomorphic observations, i.e., debris flow, landslide area, sediment deposits, etc. (Tsunetaka et al. 2020; De Haas et al. 2021). The standard workflow has been followed to generate the DEMs and orthophotos from the collected photographs (Smith et al. 2015; Saito et al. 2018; Hayakawa and Obanawa 2020; Giulietti et al. 2022; Agisoft 2022). The photograph datasets were imported into Metashape, and the 'estimate image quality' program was run for all the photographs before the image alignment. An image quality value of 0 to 1 indicates the sharpness of the photograph (Wang and Watanabe 2022), and here the photographs with a value >0.7 were used for subsequent processing. Here, some unnecessary photographs (e.g., repeated photographs) were deleted to reduce the processing work. Distorted pictures resulting from the windy conditions on the flight day and water surface reflectance limit the image alignment in data processing (Hinge et al. 2019). Here, original UAV image coordinates obtained by uncorrected single positioning of the aircraft GNSS receiver were used for image alignment. After that, image alignment of medium quality was applied to generate the point clouds. Then these point clouds were further processed to generate high-resolution DEMs (as new DEM) and orthorectified images at the WGS 1984 (UTM Zone 46N) coordinate system. We adopted this approach because of the unavailability of external GNSS receiver station, ground control point (GCP), referenced map, and difficulty in accessing possible check points locations in the land-side area. We needed extensive locations along the survey site to place if the check points or GCPs were to be placed for reducing model error (James and Robson 2012; Hayakawa and Obanawa 2020), but the accessibility was quite limited (Figure 1F-G). The error of generated DEM in the absence of GCPs mostly comes from rational function model error and may impact the accuracy of generated DEM (Wang et al. 2019). The characteristics of UAV surveys and the generated DEMs and orthorectified images are given in Table 1.

The NASADEM_HGT (30m, void-filled), created by the NASA-MEaSUREs program and publicly released in February 2020, have been downloaded for the area of interest from the NASA-LPDAAC (Land Processes Distributed Active Archive Center) website (available at https://earthexplorer.usgs.gov/) (NASA JPL 2020; Buckley et al. 2020). The necessary processing including mosaicking, raster projection, and clipping of acquired data have been performed in ArcGIS (ESRI). This study selected NASADEM (as reference surface or old DEM of 1999) from global DEMs products because it is relatively new and considered as the most accurate compared to other freely available DEM datasets, e.g., ASTER, AW3D30, MERIT, SRTM, and TanDEM-X (Franks et al. 2020; Uuemaa et al. 2020; Li et al. 2020; Tran et al. 2023; Faisal and Hayakawa 2023). It is reprocessed from the radar-based SRTM 1999 (Farr et al. 2007) with many improvements to its quality, notably void reduction and artifacts removal through improved phase unwrapping using auxiliary data from various datasets such as ASTER GDEM, PRISM (Panchromatic Remote-sensing Instrument for Stereo Mapping), GLAS (Geoscience Laser Altimeter System), and ICESat (Ice, Cloud, and Land Elevation Satellite) in processing techniques (Crippen et al. 2016, Buckley et al. 2020; Oguchi et al. 2022; Tran et al. 2023). The vertical accuracy of NASADEM has been revealed as 5.3 m (USA) (Buckley et al. 2020), 6.39 m (Estonian) (Uuemaa et al. 2020), 6.59 m (China) (Li et al. 2022), 12.08 m (New Zealand) (Uuemaa et al. 2020), and 12.6 m (Tibetan Plateau) (Chen et al. 2022). Furthermore, the NASA Jet Propulsion Laboratory (creators of the dataset) claims that the radar does an excellent job of penetrating the vegetation canopy, so the digital terrain model (DTM) bias is not significant (Franks et al. 2020).

2.3 DEM of difference (DoD) and volumetric estimates

The differencing of sequential DEMs to create a DEM of difference (DoD) is particularly relevant to geomorphic studies because a DoD may provide spatially distributed surface model of topographic and volumetric change over time (James et al. 2012). Recently, the DoD maps have been widely used in various studies regarding sediment transport, erosion volume estimation, landslides, and earthflow (Rumsby et al. 2008; Tseng et al. 2013; Hsieh et al. 2016; Hayakawa and Obanawa 2020; Wang and Watanabe 2022). In this study, DoD maps have been produced for two cross-sections over the study area. For this, the fine-resolution UAV-DEMs (0.10 m & 0.11 m) have been resampled to medium-resolution (30 m) products for the homogeneity of the resolution by using bilinear interpolation method (Tang et al. 2019). Then, two sets of DEMs (UAV-DEM & NASADEM) are transformed into WGS 1984 (UTM Zone 46 N) coordinate system for subsequent analysis. Here, the DoD maps are prepared by subtracting the earlier terrain elevation (NASADEM of 1999) from the later one (UAV-DEM of 2022) using the raster calculator in ArcGIS (Hsieh et al. 2016; Watson et al. 2019; Wang and Watanabe 2022). A level of significant change detection (LoD) was determined to filter out uncertain topographical change and considered for subsequent volumetric change analysis (Wheaton et al. 2010; Milan et al. 2011).

The standalone Geomorphic change detection (GCD) 7.5.0 tool (available at https://gcd.riverscapes.net/) is used to estimate volumetric changes (Wheaton et al. 2010), which is widely applied for quantifying the spatial pattern of geomorphic changes (James et al. 2012; Kaliraj et al. 2017; Rajakumari et al. 2022). In volume change estimations, the negative values indicate erosion and positive values indicate deposition (Corsini et al. 2009; Hsieh et al. 2016; Yang et al. 2021), where the volume estimation error can also be gained, as shown in Table 2.

2.4 Cross-sectional profile

The terrain profile is a standard analytical method to discuss terrain evolution and provides valuable information about a landscape responding to a changing base level (Kirby and Whipple 2001; Wobus et al. 2006). Here, profile extraction analysis has been conducted with the DEMs (NASADEM of 1999 and UAV-DEM of 2022) to identify the changes in topographic features across the two river cross-sections through ArcGIS environment (Hsieh et al. 2016; Cirillo 2020). For the straight-line profiling method, the starting and ending points were first selected, and elevation values between the points were calculated to generate the terrain profile based on the distribution of elevations. The results were then used to better understand the dynamic changes of river elevation and sedimentation pattern (erosion/deposition) on the floodplain over the years.

3. Results

3.1 UAV DEMs resolution and error

The main characteristics of the UAV-generated DEMs of two cross-sections is provided in Table 1. The resolution of the created DEMs in this study was 0.10 m and 0.11 m at CS-1 and CS-2, respectively with orthorectified images of 0.04 m. The generated DEMs assessed a relative camera position error of 5.24 m and 6.35 m in CS-1 and CS-2, respectively which were processed using original UAV image georeferencing. The generation of high-quality DEM in inaccessible areas without GCPs has been applied in many studies (Wang et al. 2019) but the optimized sparse point cloud with identifiable GCPs across the study sites would improve the quality of a generated model (James et al. 2017).

Table 1: Characteristics of the UAV survey and generated DEMs in study sites

Survey sites	Platform	Sensors	Flight altitude (m)	Total flight duration (min)	Images taken	DEM resolution (m)	Orthorectified image resolution (m)
CS-1	UAV (DJI MAVIC 2 PRO)	1 inch CMOS (effective pixels: 20MP, 35 mm f 2.8 lens with a 77° FOV)	120	37	775	0.10	0.04
CS-2			120	53	1050	0.11	0.04

3.2 DEM of difference (DoD)

The terrain elevation change from two periods of DEM data is presented in Table 2. The mean elevation difference for CS-1 and CS-2 is −5.23 m and −84.66 m, respectively. The DoD maps (Figure 3) at river cross-sections over time represent the spatial pattern of geomorphic change. Here, the negative values stand for the decrease in terrain elevation in these images, which may have occurred from surface erosion. On the other hand, positive values represent an increase in terrain elevation, which may be due to surface deposition. Through the DoD images presented here, the terrain evolution of the river channel can be observed. Also, the DoDs have been used here to quantitatively estimate the volumetric changes that are related to the sediment budgets. However, the elevation changes signal (larger than ±50 m) derived from the DoD maps may be affected by the artifacts, i.e., scratches on the photographs, but not sensitive to the measurements of volumetric change when varied above this threshold (Schwat et al. 2023).

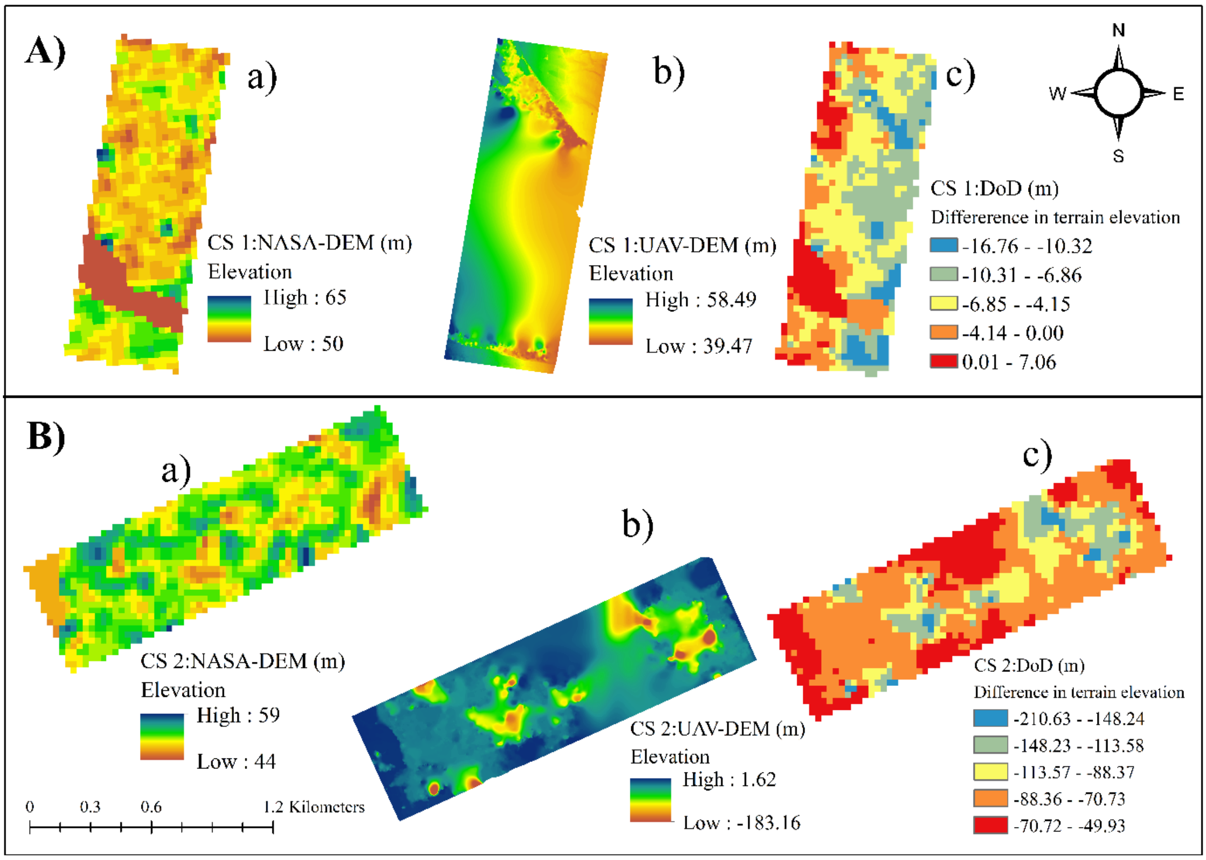

Figure 3: DEMs and DoD maps are generated from NASADEM 1999 and UAV-DEM 2022 for CS-1 (A) and CS-2 (B).

3.3 Volume estimation

The total volumes of erosion and deposition, together with the net volume change, including errors, are given in Table 2. During the period (1999-2022), the estimated erosion and deposition volumes were 4.30 million m^3 and 0.18 million m^3, respectively, in CS-1. Instead of neglecting the estimation error and supplementary debris, at least 4.30 million m^3 of sediment may have eroded from the upstream sources to this CS-1. On the other hand, at CS-2, about 86.25 million m^3 of erosion are estimated. The result indicates that erosion was the dominant process in the Teesta River floodplain, with lower deposition over the study period. The estimate of net volumetric change is CS-2 is higher than the CS-1. The estimated erosion in these two cross-sections suggests this river's dominancy of erosional features aggravated by monsoonal flow, as the UAV survey was conducted in monsoon season. The negative net volumetric change for these two sites indicates that the earthflow from the upstream should be the main source of the sediments and result in high erosion. Besides, apart from the natural upstream fluvial-sedimentation processes, this floodplain is continuously facing various anthropogenic modifications like channelization and regulations of normal river flow, channel diversion, and installation of numerous hydroelectric projects (Goyal and Goswami 2018; Higgins et al. 2018; Gupta et al. 2019; Faisal and Hayakawa 2023), which may significantly affect these high erosional features. Subsequently, this high erosion should be impacted by the construction of the Teesta barrage and the diversion of the channel for the irrigation project (Figure 6D), which is within the proximity of our present study sites. Also, previous studies mentioned the dominance of erosion in the last several decades because of the high rate of sedimentation and the rise of 1 m bed level every ten years in the Teesta River channel (Khan 2001; Akhter et al. 2019; Sultana 2022a). Furthermore, volumetric changes estimation based on the Teesta River's bathymetric survey conducted by Bangladesh Water Development Board-2011 supports our study's observation of erosional dominancy along the present study sites (BWDB 2011; Tarannum et al. 2018).

From this study, it is not possible to find real-time data on the discharge events that caused these huge erosional episodes. Therefore, it is unpredictable when and where the next discharge will occur. However, it can be mentioned that the monsoonal flow patterns control the erosional and sedimentation processes in such a large transboundary river basin. The net volume of change is often used as a sediment budget term in sediment dynamics studies. Therefore, estimating the volumetric change from the change detection can be helpful to develop a morphological sediment budget to infer the rates of sediment transport for the studied river (James et al. 2012).

Table 2: DEM difference and volumetric changes in the study sites

Study sites	DEM difference*	Mean elevation difference (m)	Standard deviation	Erosion		Deposition		Volume change (m^3) ($\times 10^6$)
				Area (m^2)	Volume (m^3) ($\times 10^6$)	Area (m^2)	Volume (m^3) ($\times 10^6$)	
CS 1	UAV DEM– NASA DEM	–5.23	3.98	688,957	4.30 ± 0.13	106,530	0.18 ± 0.02	−4.11±0.15
CS 2		–84.66	13.98	1,010,101	86.25 ± 0.18	0	0	–86.25±0.20

* The NASADEM and UAV-DEM represent the topography of 1999 and 2022, respectively.

3.4 Topographic features in the river sites

Figure 4 shows the high-resolution topographic products (slope gradient) of two cross-sections. The river flow path and the bankline in the study sites, presenting a flatland appearance, can be easily identified from the DEM maps. Most of these two cross-sections sloped eastwardly, where the slope gradient was below 5°, determining the presence of flat areas. On the other hand, the slope gradient around the bankline or near the char lands (locally known as Char) exceeds 20°. The orthomosaic images generated from the study (Figure 4) visualize the agricultural lands along the bank lines, with some human settlements that were not permanent. Due to the main river course changes, bankline erosion is widespread in the study sites, and therefore the sediments accumulated at the lower flat area.

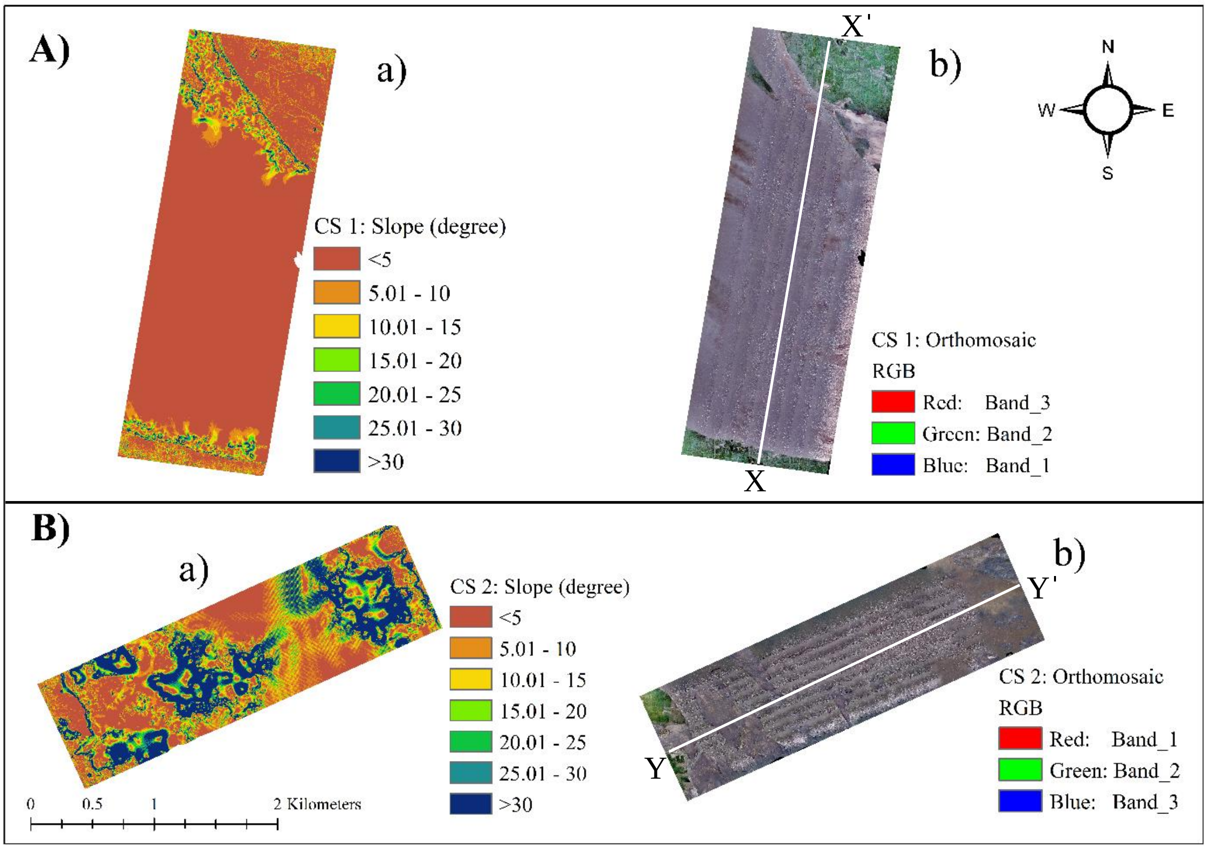

Figure 4: Slope gradient and orthomosaic images of CS-1 (A) and CS-2 (B) created from UAV photographs. See Figure 5 for the cross-sectional profiles denoted here.

3.5 Cross-sectional profile analysis

Next to elevation and volumetric change estimates, the DEMs are helpful for evaluating profiles of river cross-sections. In our study, NASADEM 1999 has been used as the reference for the profile analysis. The selected transects from two river cross-sections illustrate the profile analysis, indicating an ongoing erosion process. Figures 4A (X-X') and 4B (Y-Y') indicate the transect locations on the orthomosaic of 2022 for profile analysis. Figure 5 (A-B) shows the elevation profiles for these transects derived from the DEMs, indicating the deepening of the river channel within this period (1999-2022) with approximate errors.

Here, active sedimentation and erosion processes are significantly visible near the left bank side from the cross-sectional profiles, though several meters of uncertainty may exist.

The relative elevation change demonstrated the erosion variations within the profile position. The erosion process is relatively small for profile (A), with approximately 7 m elevation change at the lower middle section in CS-1. On the other hand, the higher erosion is visible at the profile (B), in CS-2. The Teesta barrage and diversion of the river channel for irrigation and sand extraction for financial benefit at the upper part of CS-2 may aggravate this high erosion process. Also, the bed scours depth of more than 13 m was reported at Teesta River in Nilphamari (present study site) by the Institute of Water and Flood Management (IWFM-BUET 2018-2022) (Mondal 2022), which was estimated up to 40 m in the Brahmaputra River channel (locally known as Jamuna River) (Ashworth et al. 2000), supports the erosion processes observed here. Furthermore, the multi-temporal satellite remote sensing (MSS/TM/ETM+/OLI)-based and bathymetric survey-based study explored that erosion, sand bar development, and channel shifting rate towards the left side bank has increased over a 46-year period (1972-2017) along the study sites because of the high rate of sedimentation (BWDB 2011; Akhter et al. 2019; Mondal 2022). Besides, high erosive conditions (15.32 to 31.72 km^2) that caused the bank failure were evident over the decades in several cross-sections of the Teesta River floodplain in the Nilphamari district, including our study sites (Tarannum et al. 2018; Sultana 2022a).

Nevertheless, it should be mentioned that considerable uncertainty remains in channel depth due to the glitter, over-estimation of water level, data processing software, resolution difference, and mirroring effects of water, which may affect the interpretations of these profiles (Schwanghart and Scherler 2017; Hemmelder et al. 2018). In general, the elevation error ranges from 5-12 m for NASADEM (Buckley et al. 2020; Uuemaa et al. 2020; Li et al. 2022; Uuemaa et al. 2020; Chen et al. 2022; Tran et al. 2023), whereas the UAV's single positioning of GNSS may provide error of ~8-13 m or more (DoD 2020; Elkhrachy, 2021; de Haas et al. 2021; Grunwald et al. 2023). Hence, this error and recent studies necessitate improving the accuracy of elevation data with modern UAVs connected to RTK global navigation satellite systems in the most remote and challenging geographic locations, like this study area (Elkhrachy 2021; De Haas et al. 2021).

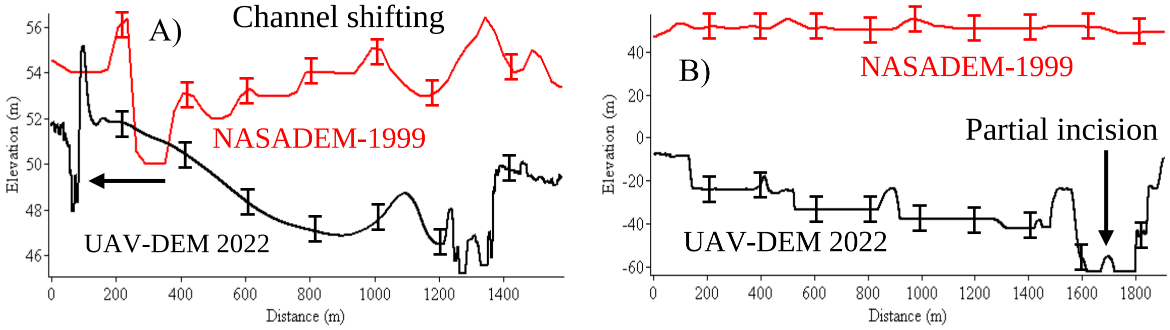

Figure 5: Changes in cross-sectional profiles. Here, A) and B) corresponds to the CS-1 (X-X' transect) and CS-2 (Y-Y' transect) shown in Figure 3. The red and black lines indicate the elevation profile of NASADEM 1999 and UAV-DEM 2022, respectively, with approximate errors (>10 m).

4. Discussion

4.1 Topographical and morphological dynamics

This paper presents a study using DEMs to map topographic changes and associated morphological dynamics, including elevation differencing, volumetric change estimates, and river cross-sectional profiles, in an understudied region where repetitive topographic measurement is absent. The availability of high-resolution river topographic data, possible through UAVs and global DEM products, allows performing topographical change detection analysis over the years (1999-2022). Nevertheless, this information is critical to understanding the river's topographical and morphological dynamics that are prone to repeated sediment disasters from its upper basin sediment flux. Furthermore, topographic factors affect the sediment discharge in a river basin (Cheng et al. 2017). Therefore, the DoD difference between the UAV-DEM and NASADEM for the area of interest (Table 2) shows the benefit of conducting UAV surveys even if ground control point is unavailable due to inaccessibility to field sites.

This study noticed the decrease of elevation from –5.23 to –84.66 m and net volumetric difference of –4.11 to –86.25 million m^3 in CS-1 and CS-2 on Teesta River's left side bank. The sedimentation between these periods varied largely per cross-section towards the left side bank of this river and seemed to dominate with the erosional process. The volume changes over the 1999–2022 periods are mainly expedited by the anthropogenic modifications of the main river channel, such as the construction of the Teesta barrage, channel diversion for irrigation, and sand mining observed from the field investigations (Figure 6). Furthermore, earlier studies documented the increase of erosion at Teesta barrage’s proximity (Khan 2001; Sultana 2022a; Mondal 2022). The visual observations on the land-side of these cross-sections (Figure 6A) also support the feasibility of such a large amount of erosion processes. Hence, using DoD derived from the DEMs has proven helpful in identifying the sedimentation pattern resulting from erosion and deposition scenarios in the floodplain. The volumetric dynamics studies prefer the DEMs from the same data source for more accurate estimations, which may affect the assessment here (Tang et al. 2019).

However, the availability of high-resolution data (same source and similar accuracy level) derived from the UAV is often not available in this region. The topographical changes recorded over the period (years 1999–2022) revealed significant variations of the topographic profile dominated by erosional process. The interaction of upstream fluvial incision, high and low discharge patterns, base-level change, and anthropogenic stressors (e.g., channelization, sand mining, and hydroelectric projects-3405 MW installed of over 8000 MW potentiality, and hydro-engineering structures) may result in the changes along these profiles (Montgomery and Brandon 2002; Goyal and Goswami 2018; Van Denderen et al. 2022). Since river cross-sectional profiles preserve valuable information on landscape evolution and are fundamental to understanding the river morphological changes, this profile analysis can be helpful in monitoring the sedimentation patterns and management of the disaster-prone landscape.

Over the years, the flashy and unpredictable nature of sedimentation in this river basin left the inhabitants in a more risky situation. Also, the sudden release of huge volumes of water from the upstream reservoir makes the sediment pattern more unpredictable and more uncertain floods in this region in recent decades (Mondal and Islam 2017). The erosion dominated sedimentation pattern and enormous volumetric changes may affect the bankline stability, development of mid-channel sand bars (locally known as char) (Figure 6B), and multithreaded channel system in Teesta River (Akhter et al. 2019; Sultana 2022a). The increased number of mid-channel bars led to the sudden shifting of the channel (Ghosh 2014), where Teesta's channel shifted towards the right (0.34 km/year) and left side (− 0.14 km/year) over the period (1972-2017) (Akhter et al. 2019). The sedimentation patterns may control the channel dynamics because the river discharge flow through the narrower channel increases the flow velocity, resulting in abrupt bank erosion (Graf 2000; Croke et al. 2008). Furthermore, the active bank erosion is causing the dislocation of the human population through seasonal (53.1%) and temporary migration (46.9%) for livelihoods in the floodplains of the Teesta River (Elahi et al. 1991; Islam 2016; Sultana 2022b). Besides, the river bank erosion aggravated by anthropogenic interventions (upstream's artificial damming, barrage, channel diversion, and controlled discharge, etc.) along this floodplain over the years has significantly affected agricultural production (rice, wheat, potato, etc.) and altered cropping practices or crop calendar (Syed et al. 2017; Faisal et al. 2019; Sultana 2022b). These have made the local community more vulnerable to food security, as half of the households (54%) depend on farming in this floodplain (Elahi and Ara 2008; BBS 2010; Syed et al. 2017).

Moreover, the excessive and unplanned extraction of sand (Figure 6C) from the sand-dominated bed profile (approximately 10 m) in the study sites has been common practice (Biswas et al. 2018). That may also alter the river morphological characteristics such as channel incision (Rai et al. 2019), changes in river bed (Best 2019), erosion of river banks (Bravard et al. 1997), and decrease of sediment flux at downstream of the river delta (Anthony et al. 2015). The channel incision process is a gradual geomorphological phenomenon. But, the point of concern is that the pace of incision may significantly be expedited from the excessive sand mining, which may result in drastic morphological changes within 10-100 years in its natural course where such changes would have occurred over millennia (Simon and Rinaldi 2006; Rai et al. 2019).

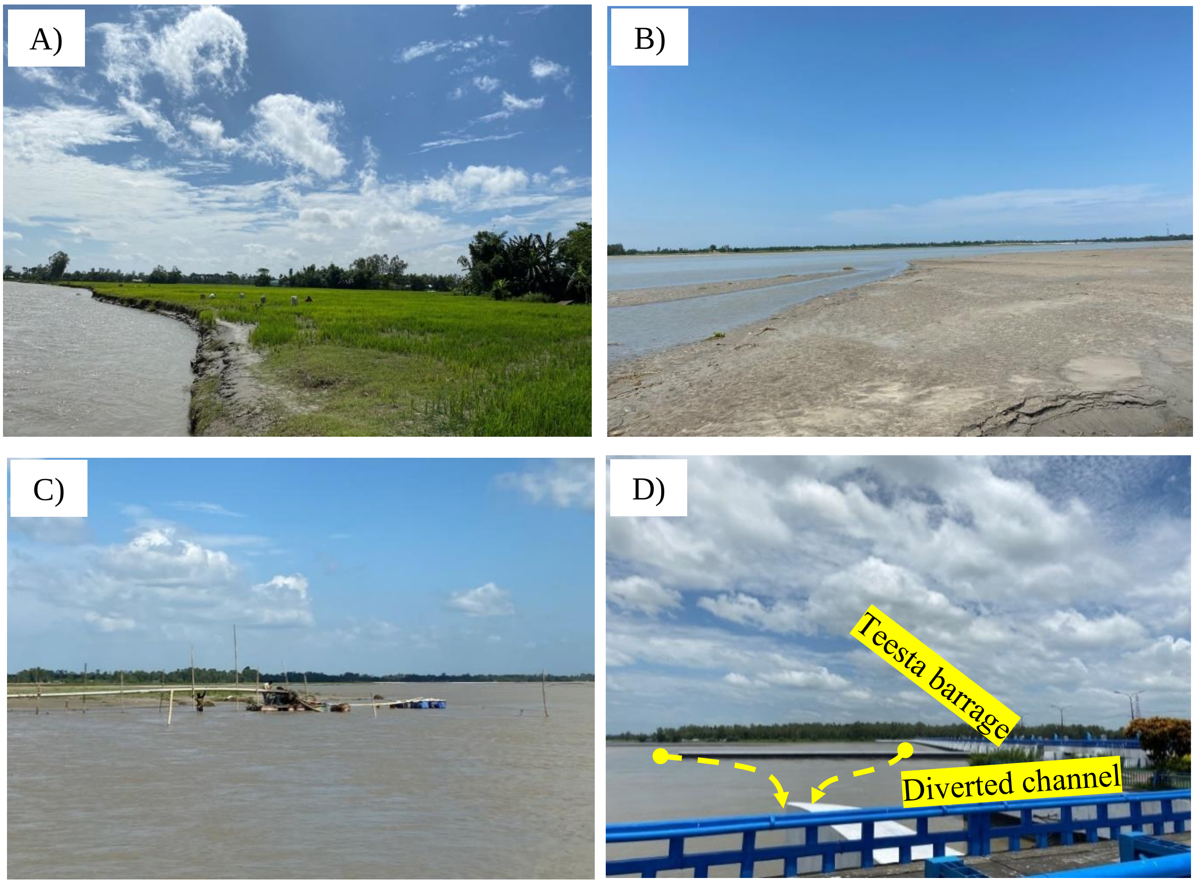

Figure 6: A) Erosion along the bank, B) sedimentation within the channel and bar development C) dredging for sand extraction, and D) channel diversion for irrigation at Teesta.

4.2 High-resolution topographic baseline, limitations, and challenges

This study showed that UAV images are suitable for monitoring the changes in river topography and geomorphology in a region where high-resolution imagery is often unavailable. To the best of our knowledge, this study successfully estimates the topography using UAV-SfM in the Teesta River sites for the first time. It is evident that high-resolution DEMs derived from the present UAV survey represents an important new baseline topographic dataset for river studies considering the existing freely available global DEM dataset, e.g., NASADEMs (Watson et al. 2019; Tang et al. 2019).

The availability of real-time kinematic (RTK) enabled UAVs in developing countries like Bangladesh will further improve the survey data and, at the same time, reduce the requirements for extensive ground control point surveys in inaccessible riverine areas (Fazeli et al. 2016; Forlani et al. 2018). With the limited scope, we only conducted UAV topographic survey single time to generate high-resolution DEMs and then used the existing medium-resolution global DEMs to analyze the topographic change due to the unavailability of high-resolution multitemporal DEMs. Hence, data obtained from different DEM generation techniques and the resampling processes to homogenous resolution (high-resolution to medium resolution) may lead to estimation errors or uncertainty, which would eventually impact the topographic change analysis (Joerg and Zemp 2014). Besides, due to the unavailability of good control points like cross marks on the road, permanent features, or the referenced maps, this study relies on the aircraft's GNSS errors to estimate the uncertainty of the UAV-generated DEMs, which were several meters. Besides, this topographic study did not consider the monsoonal effect, which is one of the limiting factors raised by the study's limited scope. Some approximations, such as the presence of water bodies in the riverbed, water surface reflectance, and differences in DEM sources and resolution, may also constrain our analysis. Nevertheless, we believe that such approximations would not dramatically influence the analysis and the interpretations.

The availability of RTK-enabled aircraft, external GNSS receiver, and evenly distributed ground control points with geographical coordinates were challenging, but addressing these issues may improve the elevation data quality. Furthermore, some key challenges remain in UAV-based riverine floodplain monitoring, such as wind, rain, surface reflectance, image focus, image resolution, and processing equipment (Hashemi-Beni et al. 2018; Acharya et al. 2021). Besides, a quantitative assessment of the accuracy and precision of the UAV-derived products compared to RTK-GPS-enabled UAV and terrestrial laser scanning (TLS) are beyond the scope of this paper. Though, it is expected that the topographic data acquired via TLS would be more accurate compared to SfM-derived products in geomorphic investigations (Tsunetaka et al. 2020). Furthermore, UAV survey and high-resolution DEM generation techniques may also attract attention to the research community in that region. Where the applicability of advanced remote sensing techniques (such as UAV-SfM and LiDAR) for geomorphological investigation is very limited compared to neighboring countries like China (Le Heron et al. 2019), India (Ramsankaran et al. 2020; Dhote et al. 2022), Bhutan (Dunning et al. 2009; Tempa et al. 2021), Nepal (Immerzeel et al. 2014; Kraaijenbrink et al. 2016; Van Woerkom et al. 2019), Pakistan (Khan et al. 2021), and in other parts of the worlds (Śledź et al. 2021).

4.3 Advances in river floodplain management

Evaluating recent topographic change in a riverine environment relevant to the sustainability of human populations in the disaster-prone area requires up-to-date fine-resolution DEMs, such as those derived using UAV imagery in this study. In our case, single-time UAV image acquisitions and use of global DEM products for volumetric change estimate along the river cross-sections are low to link sedimentation patterns. In this context, the high temporal UAV data acquisition campaigns after each important discharge event or season scale can provide important information regarding the river sedimentation pattern and hence the management of sediment disasters in these disaster-prone deltaic landscapes. The processing of hundreds or thousands of images using the SfM algorithm is computationally intensive but fast, straightforward, and produces detailed results (Clapuyt et al. 2016; Hemmelder et al. 2018). With the advancement of UAV developments and innovations, UAV operations are becoming easy to monitor the river floodplain. Despite some challenges in river topographic measurement, UAV-based DEM should be considered as the optimal choice for investigations over river floodplains due to its advantages of portability, high data processing speed, low flying height, convenient flying preparation, and the ease of generating orthoimage and DEM data (Hayakawa and Obanawa 2020).

Despite some limitations and challenges, the current approach of terrain evaluation utilizing free and on-demand DEMs can be helpful for other areas where repetitive terrain information is scarce but requires effective topographic investigation. Furthermore, land managers and mapping agencies responsible for monitoring river dynamics and management could use the methods presented in this paper, especially the UAV-SfM data generation techniques for the advancement of river floodplain management. The effective monitoring requires sufficient knowledge of fluvial-sedimentation processes in the riverine floodplain, and in this regard, encouragement can be taken from fluvial research advancement mentioned by Stott (2013), Wohl (2014), Piégay et al. (2015), and Oguchi et al. (2022). In the advancement of riverine floodplain management, the UAV-SfM photogrammetry can be an effective and powerful tool to map morphological dynamics and processes focusing on the river basin maintenance plan, delineation of flood-prone areas (Şerban et al. 2016), estimation of flood volume and extent (Escobar Villanueva et al. 2019), flood risk modeling (Coveney and Roberts 2017), assessing the impact of flooding (Langhammer and Vackova 2018), sediment discharge analysis, hydro-engineering site suitability (i.e., dredging, sand mining), and responding to fluvial disasters and emergencies (i.e., GLOFs) (Salmoral et al. 2020; Sattar 2023; Chauhan 2023).

Furthermore, understanding river topographic and related morphological dynamics will promote the development of a river floodplain management framework, where the studies of Morris-Oswald and Sinclair (2005), APFM (2012); Kiedrzyńska et al. (2015), Sharma et al. (2019), Serra-Llobet et al. (2022), and Chan et al. (2022) can be exemplary. The existing river floodplain management approaches in transboundary river (total 57 rivers) dominated Bangladesh should not focus on the traditional hard engineering approach (Haque et al. 2019), which may not be enough to mitigate substantial risks from the natural (e.g., climate change, sea-level rise, and land subsidence) and anthropogenic factors (e.g., channelization, hydro-engineering structures, excessive sand mining, large population, and rapid socio-economic growth) (Chan et al. 2022). Hence, repetitive topographic data collection through the RTK-enabled UAVs at seasonal (pre-and post-monsoon) and temporal scales or event-based in future studies would be significant for this disaster-prone deltaic region, particularly estimation of flood volume and extent, river bank erosion, seasonal dredging, and site-specific sand mining, following the frameworks mentioned in Figure 7. Therefore, the advancement of river management needs to focus on collaborative projects (Hayakawa et al. 2017; Ogura et al. 2023) focusing on utilizing the UAV-based framework to support decision-making in hazard assessments and emergency responses in the disaster-prone landscape of South Asia, particularly Bangladesh.

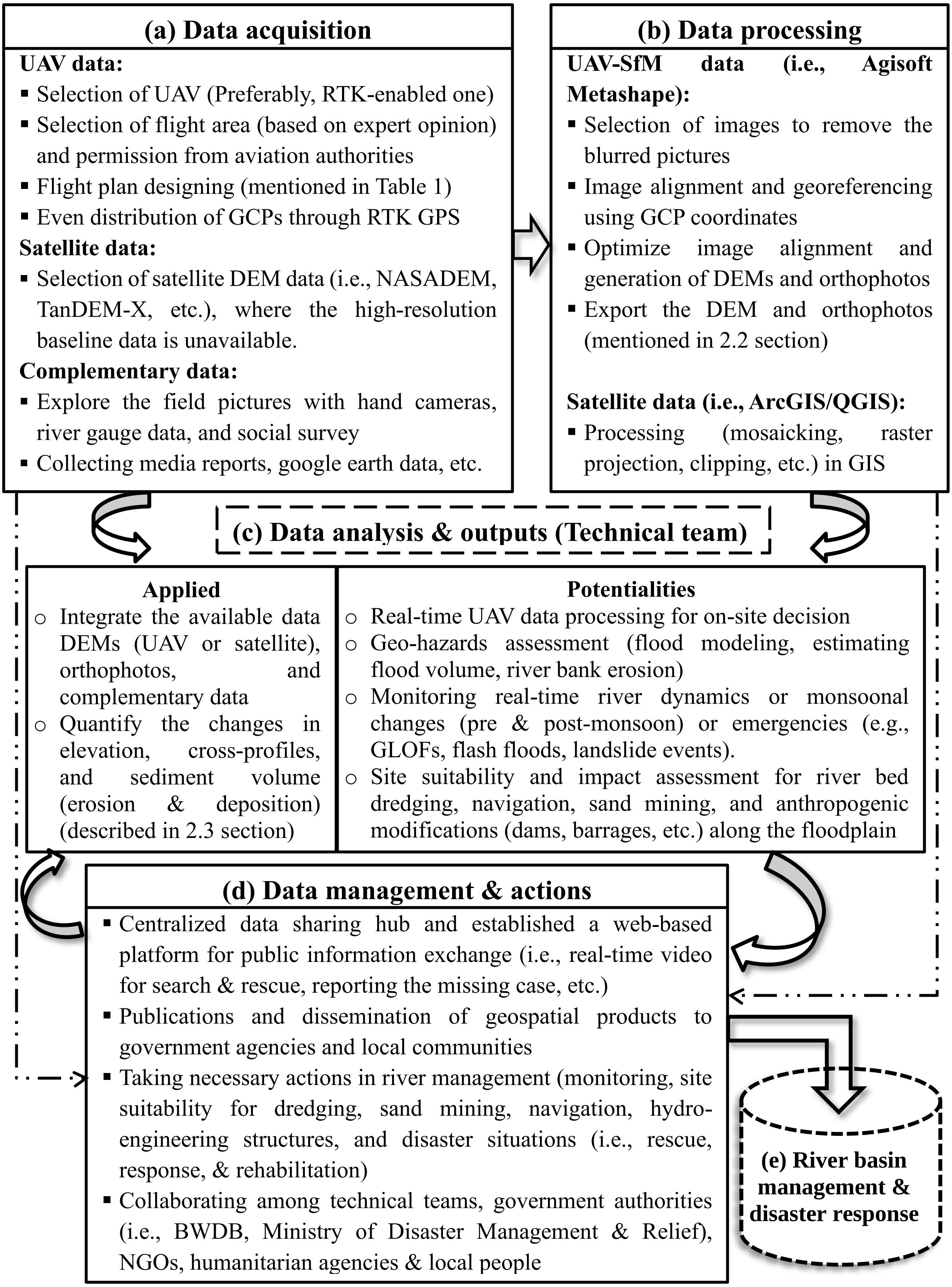
(a) Data acquisition
UAV data:
▪ Selection of UAV (Preferably, RTK-enabled one)
▪ Selection of flight area (based on expert opinion) and permission from aviation authorities
▪ Flight plan designing (mentioned in Table 1)
▪ Even distribution of GCPs through RTK GPS
Satellite data:
▪ Selection of satellite DEM data (i.e., NASADEM, TanDEM-X, etc.), where the high-resolution baseline data is unavailable.
Complementary data:
▪ Explore the field pictures with hand cameras, river gauge data, and social survey
▪ Collecting media reports, google earth data, etc.
(b) Data processing
UAV-SfM data (i.e., Agisoft Metashape):
▪ Selection of images to remove the blurred pictures
▪ Image alignment and georeferencing using GCP coordinates
▪ Optimize image alignment and generation of DEMs and orthophotos
▪ Export the DEM and orthophotos (mentioned in 2.2 section)
Satellite data (i.e., ArcGIS/QGIS):
▪ Processing (mosaicking, raster projection, clipping, etc.) in GIS
(c) Data analysis & outputs (Technical team)
Applied
o Integrate the available data DEMs (UAV or satellite), orthophotos, and complementary data
o Quantify the changes in elevation, cross-profiles, and sediment volume (erosion & deposition) (described in 2.3 section)
Potentialities
o Real-time UAV data processing for on-site decision
o Geo-hazards assessment (flood modeling, estimating flood volume, river bank erosion)
o Monitoring real-time river dynamics or monsoonal changes (pre & post-monsoon) or emergencies (e.g., GLOFs, flash floods, landslide events).
o Site suitability and impact assessment for river bed dredging, navigation, sand mining, and anthropogenic modifications (dams, barrages, etc.) along the floodplain
(d) Data management & actions
▪ Centralized data sharing hub and established a web-based platform for public information exchange (i.e., real-time video for search & rescue, reporting the missing case, etc.)
▪ Publications and dissemination of geospatial products to government agencies and local communities
▪ Taking necessary actions in river management (monitoring, site suitability for dredging, sand mining, navigation, hydro-engineering structures, and disaster situations (i.e., rescue, response, & rehabilitation)
▪ Collaborating among technical teams, government authorities (i.e., BWDB, Ministry of Disaster Management & Relief), NGOs, humanitarian agencies & local people
(e) River basin management & disaster response

Figure 7: Framework for river basin management and natural disaster with UAVs

5. Conclusions

This study demonstrates the utility of an integrated geographic information system combined with UAV-SfM-derived DEMs and globally available DEMs (NASADEM), considering topographical and geomorphological dynamics in a disaster-prone riverine floodplain. The workflow presented here has been successfully applied to identify the topographic and geomorphic changes, as well as assess the sedimentation pattern in the river channel based on multiple topographic outputs (DEMs, DoDs, cross profiles). We noticed the changes in elevation (−5.23 to −84.66 m), sediment volume (−4.11±0.15 to −86.25±0.20 million m^3), and erosion-dominated cross-sectional profiles towards the left side bank in the transboundary Teesta River over a period of 23 years (1999-2022). The current approach of data acquisition, especially the UAV-SfM-derived DEMs and orthomosaic images, can encourage interested researchers to take this study as baseline information for future investigation, where the UAV data can be available on request to the authors. In addition, time series investigations with advanced remote sensing techniques (such as UAV-SfM and LiDAR etc.) for detailed monitoring of topographic variables considering the monsoonal dynamics are essential to assess future instability scenarios in this dynamic, unpredictable, and disaster-prone river floodplains. The findings from this study will provide a better understanding of the river's topographical dynamics, geomorphological processes, and sedimentation scenario to national-river managers. Also, the proposed river basin management framework will elevate river floodplain management and disaster response in South Asia’s densely populated deltaic landscape, particularly Bangladesh and/or similar situations elsewhere.

List of abbreviations

ASTER: Advanced Spaceborne Thermal Emission and Reflection satellite

AW3D: ALOS Global Digital Surface Model

BWDB: Bangladesh Water Development Board

DEMs: Digital Elevation Models

DoD: DEM of Difference

DTM: Digital Terrain Model

DRONE: Dynamic Remotely Operated Navigation Equipment

EGM96: Earth Gravitational Model 1996

ESRI: Environmental System Research Institute Inc.

GBM: Ganges-Brahmaputra-Meghna

GCD: Geomorphic Change Detection

GCPs: Ground Control Points

GLAS: Geoscience Laser Altimeter System

GLONASS: Global Navigation Satellite System

GLOFs: Glacial Lake Outburst Flood

GNSS: Global Navigation Satellite System

HAE: Height Above Ellipsoid

ICESat: Ice, Cloud, and Land Elevation Satellite

LiDAR: Light Detection and Ranging

LPDAAC: Land Processes Distributed Active Archive Center

MEaSUREs: Making Earth System Data Records for Use in Research Environments

MERIT: Multi-Error-Removed Improved-Terrain

NASADEM: National Aeronautics and Space Administration DEM

PRISM: Panchromatic Remote-sensing Instrument for Stereo Mapping

RTK: Real-Time Kinematic

SfM-MVS: Structure from Motion Multiview Stereo Workflow

SRTM: Shuttle Radar Topography Mission

TanDEM-X: TerraSAR-X add-on for Digital Elevation Measurement

TLS: Terrestrial Laser Scanning

UAVs: Unmanned Aerial Vehicles

Acknowledgements

This work was supported by the Ministry of Education, Culture, Sports, Science and Technology (MEXT) scholarship. We are grateful to Professor Mohammed Jamal Uddin (Jahangirnagar University, Bangladesh), Md. Abul Kashem Majumder (Hydro-geologist), and Bangladesh Water Development Board for their kind assistance in the field investigation. We are grateful to the editorial team, particularly Karin Ebert and anonymous reviewers for their

constructive comments and insightful suggestions, which significantly improved our manuscript.

References

Acharya BS, Bhandari M, Bandini F, Pizarro A, Perks M, Joshi DR, Wang S, Dogwiler T, Ray RL, Kharel G. 2021. Unmanned aerial vehicles in hydrology and water management: applications, challenges, and perspectives. Water Resour. Res. 57 (11), e2021WR029925. https://doi.org/10.1029/2021WR029925

AgiSoft PhotoScan Professional (Version 1.8.1 Build 13915, 64 bit) [Software]. 2022. Available online: https://www.agisoft.com/pdf/metashape-pro_1_8_en.pdf (accessed on 29 Sep 2022).

Akhter S, Eibek KU, Islam S, Islam ARMT, Chub R, Shuanghe S. 2019. Predicting spatiotemporal changes of channel morphology in the reach of Teesta River, Bangladesh using GIS and ARIMA modeling. Quatern. Int. 513:80–94. https://doi.org/10.1016/j.quaint.2019.01.022

Alford D. 1992. Hydrological aspects of the Himalayan region. ICIMOD occasional paper 18, International Centre for Integrated Mountain Development, Kathmandu, Nepal. https://doi.org/10.53055/ICIMOD.115 (accessed on 20 Jan 2024).

Annis A, Nardi F, Petroselli A, Apollonio C, Arcangeletti E, Tauro F, Grimaldi S. 2020. UAV-DEMs for small-scale flood hazard mapping. Water 12 (6), 1717. https://doi.org/10.3390/w12061717

Anthony EJ, Brunier G, Besset M, Goichot M, Dussouillez P, Nguyen VL. 2015. Linking rapid erosion of the Mekong River delta to human activities. Sci. Rep. 5, 14745. https://doi.org/10.1038/srep14745

APFM (Associated Programme on Flood Management) 2012. Integrated flood management tools series (Issue 13): conservation and restoration of rivers and floodplains. Compiled in association with World Meteorological Organization (WMO) and the Global Water Partnership (GWP). https://library.wmo.int/doc_num.php?explnum_id=7332

Ashworth PJ, Best JL, Roden JE, Bristowà CS, Klaassen GJ. 2000. Morphological evolution and dynamics of a large, sand braid-bar, Jamuna River, Bangladesh. Sedimentology 47:533–555. https://doi.org/10.1046/j.1365-3091.2000.00305.x

Ashrafi ZM, Shuvo SD, Mahmud MS. 2016. Changes in course pattern of the Teesta River after the effect of an engineering project. AGU fall meeting abstracts, EP51A–0859. https://ui.adsabs.harvard.edu/abs/2016AGUFMEP51A0859A

Avand M, Kuriqi A, Khazaei M, Ghorbanzadeh O. 2022. DEM resolution effects on machine learning performance for flood probability mapping. J. Hydro Environ. Res. 40:1–16. https://doi.org/10.1016/j.jher.2021.10.002

BWDB (Bangladesh Water Development Board) 2011. Rivers of Bangladesh. BDWB reports in August 2011. Dhaka, Bangladesh.

BBS (Bangladesh Bureau of Statistics) 2010. Census of agriculture 2008: National series, volume 1-Structure of agricultural holdings & livestock population. Ministry of Planning, Government of Bangladesh, Dhaka, pp. 711.

BBS (Bangladesh Bureau of Statistics) 2016. Statistical year book of Bangladesh, Dhaka. http://www.bbs.gov.bd/site/page/29855dc1-f2b4-4dc0-9073-f692361112da/Statistical-Yearbook (accessed in Jan 2023).

Best J. 2019. Anthropogenic stresses on the world’s big rivers. Nature Geosci. 12:7–21. https://doi.org/10.1038/s41561-018-0262-x

Biswas PK, Ahmed SS, Pownceby MI, Haque N, Alam S, Zaman MN, Rahman MA. 2018. Heavy mineral resource potential of Tista river sands, Northern Bangladesh. Appl. Earth Sci. 127(3):94–105. https://doi.org/10.1080/25726838.2018.1488357

Bravard JP, Amoros C, Pautou G, Bornette G, Bournaud M, Creuzé des Châtelliers M, Tachet H. 1997. River incision in south-east France: morphological phenomena and ecological effects. Regulated rivers: research & management 13(1):75–90. https://doi.org/10.1002/(SICI)1099-1646(199701)13:1%3C75::AID-RRR444%3E3.0.CO;2-6

Buckley SM, Agram PS, Belz JE, Crippen RE, Gurrola EM, Hensley S, Kobrick M, Lavalle M, Martin JM, Neumann M, Nguyen QD, Rosen PA, Shimada JG, Simard M, Tung WW. 2020. NASADEM: User guide. NASA/JPL, January, California, USA. https://lpdaac.usgs.gov/documents/592/NASADEM_User_Guide_V1.pdf (accessed on March 2022)

Cai M, Gao J, Fan X, Liu S, Shen W, He C. 2022. Estimation of river discharge using Unmanned Aerial Vehicle (UAV) based on manning formula for an ungauged alpine river in the eastern Qilian mountains. Water 14(13), 2100. https://doi.org/10.3390/w14132100

Chan FKS, Yang LE, Mitchell G, Wright N, Guan M, Lu X, Wang Z, Montz B, Adekola O. 2022. Comparison of sustainable flood risk management by four countries–the United Kingdom, the Netherlands, the United States, and Japan–and the implications for Asian coastal megacities. Nat. Hazards Earth Syst. Sci. 22:2567–2588. https://doi.org/10.5194/nhess-22-2567-2022

Chauhan A. 2023. Glacial lake outburst flood kills 14 in Sikkim, 102 people missing: What is GLOF, and why does it happen? The Indian express (published on 06 October 2023, online). https://indianexpress.com/article/explained/explained-climate/glacial-lake-outburst-flood-glof-sikkim-8968562/ (accessed on 16 Jan 2024).

Cheng NN, He HM, Yang SY, Lu YJ, Jing ZW. 2017. Impacts of topography on sediment discharge in Loess Plateau, China. Quat. Int. 440 (Part B):119–129. https://doi.org/10.1016/j.quaint.2016.12.005

Chen W, Yao T, Zhang G, Li F, Zheng G, Zhou Y, Xu F. 2022. Towards ice-thickness inversion: an evaluation of global digital elevation models (DEMs) in the glacierized Tibetan Plateau, The Cryosphere 16:197–218. https://doi.org/10.5194/tc-16-197-2022, 2022.

Cirillo D. 2020. Digital field mapping and drone-aided survey for structural geological data collection and seismic hazard assessment: case of the 2016 central Italy earthquakes. Appl. Sci. 10 (15), 5233. https://doi.org/10.3390/app10155233

Clapuyt F, Vanacker V, Van Oost K. 2016. Reproducibility of UAV-based earth topography reconstructions based on structure-from-motion algorithms. Geomorphology 260:4–15. https://doi.org/10.1016/j.geomorph.2015.05.011

Corsini A, Borgatti L, Cervi F, Dahne A, Ronchetti F, Sterzai P. 2009. Estimating mass-wasting processes in active earth slides-Earth flows with time-series of High-Resolution DEMs from photogrammetry and airborne LiDAR. Nat. Hazards Earth Syst. Sci. 9:433–439. https://doi.org/10.5194/nhess-9-433-2009

Coveney S, Roberts K. 2017. Lightweight UAV digital elevation models and orthoimagery for environmental applications: data accuracy evaluation and potential for river flood risk modelling. Int. J. Remote Sens. 38(8–10):3159–3180. https://doi.org/10.1080/01431161.2017.1292074

Crippen R, Buckley S, Belz E, Gurrola E, Hensley S, Kobrick M, Lavalle M, Martin J, Neumann M, Nguyen Q. 2016. NASADEM global elevation model: methods and progress. Int. Arch. Photogramm. Remote Sens. Spatial Inf. Sci. XLI-B4:125–128. https://doi.org/10.5194/isprs-archives-XLI-B4-125-2016

Croke JC, Purvis-Smith D, Thompson CJ, Lymburner L. 2008. The effect of local- scale valley constrictions on flood inundation and catchment-scale sediment delivery in the Fitzroy River Basin, Australia. IAHS-AISH Publication, 325:200–207. https://iahs.info/uploads/dms/14514.31-200-207-25-325-Croke.pdf

Darby SE, Dunn FE, Nicholls RJ, Rahman M, Riddy L. 2015. A first look at the influence of anthropogenic climate change on the future delivery of fluvial sediment to the Ganges–Brahmaputra–Meghna delta. Environ. Sci. Process Impacts 17 (9):1587–1600. https://doi.org/10.1039/C5EM00252D

De Haas T, Nijland W, McArdell BW, Kalthof MWML. 2021. Case report: optimization of topographic change detection with UAV structure-from-motion photogrammetry through survey co-alignment. Front. Remote Sens. 2, 626810. https://doi.org/10.3389/frsen.2021.626810

DoD (Department of Defense) 2020. Global positioning system standard positioning service performance standard, (5th eds.). US Department of Defense, Arlington, TX, USA. https://www.gps.gov/technical/ps/2020-SPS-performance-standard.pdf

Dhote PR, Thakur PK, Chouksey A, Srivastav SK, Raghvendra S, Rautela P, Ranjan R, Allen S, Stoffel M, Bisht S, Negi SB, Aggarwal SP, Chauhan P. 2022. Synergistic analysis of satellite, unmanned aerial vehicle, terrestrial laser scanner data and process-based modelling for understanding the dynamics and morphological changes around the snout of Gangotri Glacier, India. Geomorphology 396, 1080052. https://doi.org/10.1016/j.geomorph.2021.108005

Dunn FE, Nicholls RJ, Darby SE, Cohen S, Zarfl C, Fekete BM. 2018. Projections of historical and 21st century fluvial sediment delivery to the Ganges-Brahmaputra-Meghna, Mahanadi, and Volta deltas. Sci. Total Environ. 642:105–116. https://doi.org/10.1016/j.scitotenv.2018.06.006

Dunning SA, Massey CI, Rosser NJ. 2009. Structural and geomorphological features of landslides in the Bhutan Himalaya derived from Terrestrial Laser Scanning. Geomorphology 103:17–29. https://doi.org/10.1016/j.geomorph.2008.04.013

Elahi KM, Rogge J. 1990. Riverbank erosion, flood, and population displacement in Bangladesh. A report on the river bank erosion impact study. Riverbank erosion impact study, Jahangirnagar University, Dhaka, Bangladesh.

Elahi KM, Ahmed KS, Mafizuddin M. 1991. Riverbank erosion, flood and population displacement in Bangladesh: an overview. In: Elahi KM, Ahmed KS, Mafizuddin M. (Eds.), River bank erosion, flood and population displacement in Bangladesh. Riverbank erosion impact study, Jahangirnagar University, Dhaka, pp. 95–109.

Elahi KM, Ara I. 2008. Understanding the Monga in northern Bangladesh. Academic press and publishers library, Dhaka, Bangladesh.

Elkhrachy I. 2021. Accuracy assessment of low-cost Unmanned Aerial Vehicle (UAV) photogrammetry. Alex. Eng. J. 60(6):5579–5590. https://doi.org/10.1016/j.aej.2021.04.011

Escobar Villanueva JR, Iglesias Martinez L, Perez Montiel JI. 2019. DEM generation from fixed-wing UAV imaging and LiDAR-derived ground control points for flood estimations. Sensors 19 (14), 3205. https://doi.org/10.3390/s19143205

ESRI ArcGIS Desktop: Release 10.7.1 [software] 2023. Environmental Systems Research Institute: Redlands, CA, USA. (accessed in October 2023).

Faisal BMR, Rahman H, Sharifee NH, Sultana N, Islam MI, Ahammad T. 2019. Remotely sensed Boro rice production forecasting using MODIS-NDVI: a Bangladesh perspective. AgriEngineering, 1(3): 356–375. https://doi.org/10.3390/agriengineering1030027

Faisal BMR, Hayakawa YS. 2022. Geomorphological processes and their connectivity in hillslope, fluvial, and coastal areas in Bangladesh: A review. Prog. Earth Planet. Sci. 9, 41. https://doi.org/10.1186/s40645-022-00500-8

Faisal BMR, Hayakawa YS. 2023. Geomorphometric characterization and sediment connectivity of the middle Brahmaputra River basin. Geomorphology 429, 108665. https://doi.org/10.1016/j.geomorph.2023.108665

Farr TG, Rosen PA, Caro E, Crippen R, Duren R, Hensley S, Kobrick M, Paller M, Rodriguez E, Roth L, Seal D, Shaffer S, Shimada J, Umland J, Werner M, Oskin M, Burbank D, Alsdorf D. 2007. The Shuttle Radar Topography Mission. Rev. Geophys 45 (2), RG2004. https://doi.org/10.1029/2005RG000183

Fanta-Jende P, Steininger D, Bruckmüller F, Sulzbachner C. 2020. A versatile UAV near real-time mapping solution for disaster response–concept, ideas and implementation. Int. Arch. Photogramm. Remote. Sens. Spat. Inf. Sci. 43:429–435. https://doi.org/10.5194/isprs-archives-XLIII-B1-2020-429-2020

Fazeli H, Samadzadegan F, Dadrasjavan F. 2016. Evaluating the potential of RTK-UAV for automatic point cloud generation in 3D rapid mapping. Int. Arch. Photogramm. Remote Sens. Spat. Inf. Sci. XLI-B6, 41:221–226. https://doi.org/10.5194/isprs-archives-XLI-B6-221-2016

Forlani G, Dall'Asta E, Diotri F, Cella UMd, Roncella R, Santise M. 2018. Quality assessment of DSMs produced from UAV flights georeferenced with on-board RTK positioning. Remote Sens. 10(2), 311. https://doi.org/10.3390/rs10020311

Franks S, Storey J, Rengarajan R. 2020. The new Landsat collection-2 digital elevation model. Remote Sens. 12(23), 3909. https://doi.org/10.3390/rs12233909

Ghosh K. 2014. Planform pattern of the lower Teesta River after the Gazaldoba barrage. Indian J. Geogr. Environ. 13:127–137.

Giordan D, Hayakawa YS, Nex F, Tarolli P. 2018. Preface: The use of remotely piloted aircraft systems (RPAS) in monitoring applications and management of natural hazards. Nat. Hazards Earth Syst. Sci. 18:3085–3087. https://doi.org/10.5194/nhess-18-3085-2018

Giordan D, Adams MS, Aicardi I, Alicandro M, Allasia P, Baldo M, De Berardinis P, Dominici D, Godone D, Hobbs P, Lechner V, Niedzielski T, Piras M, Rotilio M, Salvini R, Segor V, Sotier B, Troilo F. 2020. The use of unmanned aerial vehicles (UAVs) for engineering geology applications. Bull. Eng. Geol. Environ. 79:3437–3481. https://doi.org/10.1007/s10064-020-01766-2

Giulietti N, Allevi G, Castellini P, Garinei A, Martarelli M. 2022. Rivers water level assessment using UAV photogrammetry and RANSAC method and the analysis of sensitivity to uncertainty sources. Sensors 22(14), 5319. https://doi.org/10.3390/s22145319

Goyal MK, Goswami UP. 2018. Teesta River and its ecosystem. In: Singh D, (Eds.), The Indian Rivers. Springer Hydrogeology. Springer Nature Singapore Pte Ltd., pp. 537–551. https://doi.org/10.1007/978-981-10-2984-4_37

Graf WL. 2000. Locational probability for a dammed, urbanizing stream: Salt River, Arizona, USA. Environ. Manag. 25: 321–335. https://doi.org/10.1007/s002679910025

Grunwald G, Ciećko A, Kozakiewicz T, Krasuski K. 2023. Analysis of GPS/EGNOS positioning quality using different ionospheric models in UAV navigation. Sensors 23(3), 1112. https://doi.org/10.3390/s23031112

Gupta N, Mishra A, Agrawal NK, Shrestha AB. 2019. Potential impacts of climate change on water resources and adaptation policies in the Brahmaputra River basin. Working paper 2019/8, ICIMOD, Kathmandu, Nepal. https://lib.icimod.org/api/files/50192326-a4cb-417b-a1fd-16b170586128/icimod622_13.1.2020.pdf (accessed on 25 Jan 2024).

Haque CE, Azad MAK, Choudhury MUI. 2019. Discourse of flood management approaches and policies in Bangladesh: mapping the changes, drivers, and actors. Water 11(12), 2654. https://doi.org/10.3390/w11122654

Hashemi-Beni L, Jones J, Thompson G, Johnson C, Gebrehiwot A. 2018. Challenges and opportunities for UAV-based digital elevation model generation for flood-risk management: a case of Princeville, North Carolina. Sensors 18(11), 3843. https://doi.org/10.3390/s18113843

Hayakawa YS, Obanawa H. 2020. Volumetric change detection in bedrock coastal cliffs using terrestrial laser scanning and UAS-based SfM. Sensors 20(12), 3403. https://doi.org/10.3390/s20123403

Hemmelder S, Marra W, Markies H, De Jong SM. 2018. Monitoring river morphology & bank erosion using UAV imagery–a case study of the river Buëch, Hautes-Alpes, France. Int. J. Appl. Earth Obs. Geoinf. 73:428–437. https://doi.org/10.1016/j.jag.2018.07.016

Higgins S, Overeem I, Rogers K, Kalina E. 2018. River linking in India: downstream impacts on water discharge and suspended sediment transport to deltas. Elementa Sci. Anthr. 6, 20. https://doi.org/10.1525/elementa.269

Higano Y, Islam MF. 2002. Rural poverty alleviation through large-scale irrigation planning: Problem and prospects of the Dalia Barrage project, Bangladesh. Bulletin of Research Institute of Economic Science 32:371–384.

Hinge L, Gundorph J, Ujang U, Azri S, Anton F, Rahman AA. 2019. Comparative analysis of 3D photogrammetry modeling software packages for drones survey. Int. Arch. Photogramm. Remote Sens. Spatial Inf. Sci. XLII-4/W12:95–100. https://doi.org/10.5194/isprs-archives-XLII-4-W12-95-2019

Hsieh Y-C, Chan Y-C, Hu J-C. 2016. Digital elevation model differencing and error estimation from multiple sources: a case study from the Meiyuan Shan landslide in Taiwan. Remote Sens. 8(3), 199. https://doi.org/10.3390/rs8030199

Immerzeel WW, Kraaijenbrink PDA, Shea JM, Shrestha AB, Pellicciotti F, Bierkens MFP, De Jong SM. 2014. High-resolution monitoring of Himalayan glacier dynamics using unmanned aerial vehicles. Remote Sens. Environ. 150:93–103. https://doi.org/10.1016/j.rse.2014.04.025

Islam MF. 2016. The Teesta River and its basin area. In: Islam M. F. (Eds.), Water use and poverty reduction. Springer Tokyo, Japan. pp. 13–42. https://doi.org/10.1007/978-4-431-55172-0

Islam MS, Islam ARMT, Rahman F, Ahmed F, Haque MN. 2014. Geomorphology and land use mapping of northern part of Rangpur district, Bangladesh. Int. J. Geomat. Geosci. 2(4):145–150.

James MR, Robson S, d'Oleire-Oltmanns S, Niethammer U. 2017. Optimising UAV topographic surveys processed with structure-from-motion: ground control quality, quantity and bundle adjustment. Geomorphology 280:51–66. https://doi.org/10.1016/j.geomorph.2016.11.021

James LA, Hodgson ME, Ghoshal S, Latiolais MM. 2012. Geomorphic change detection using historic maps and DEM differencing: the temporal dimension of geospatial analysis. Geomorphology 137(1):181–198. https://doi.org/10.1016/j.geomorph.2010.10.039

James MR, Robson S. 2012. Straightforward reconstruction of 3D surfaces and topography with a camera: accuracy and geoscience application. J. Geophys. Res. 117:1–17. https://doi.org/10.1029/2011JF002289

Joerg PC, Zemp M. 2014. Evaluating volumetric glacier change methods using airborne laser scanning data. Geogr. Ann. A: Phys. Geogr. 96(2):135–145. https://doi.org/10.1111/geoa.12036

Hayakawa YS, Fujita H, Lee S, Sagara T. 2017. Developing a data-sharing system for geospatial research: A case study on the Joint Research Assist System (JoRAS). Int. J. Spat. Data Infr. 12:141–160. https://ijsdir.sadl.kuleuven.be/index.php/ijsdir/article/view/459

Kale VS. 2002. Fluvial geomorphology of Indian rivers: an overview. Prog. Phys. Geogr. 26 (3):400–433. https://doi.org/10.1191/0309133302pp343ra

Kaliraj S, Chandrasekar N, Ramachandran KK, Srinivas Y, Saravanan S. 2017. Coastal landuse and land cover change and transformations of Kanyakumari coast, India using remote sensing and GIS. Egypt. J. Remote. Sens. 20(2):169–185. https://doi.org/10.1016/j.ejrs.2017.04.003

Khan A. 2001. Morphological changes due to construction of a barrage on the Teesta River. Thesis available at: Lib.buet.ac.bd. http://lib.buet.ac.bd:8080/xmlui/handle/123456789/188 (accessed in Feb 2023).

Khan MSS, Islam ARMT. 2015. Anthropogenic impact on morphology of Teesta River in northern Bangladesh: an exploratory study. J Geosci. Geomat. 3(3):50–55. http://pubs.sciepub.com/jgg/3/3/1

Khan MY, Shafique M, Turab SA, Ahmad N. 2021. Characterization of an unstable slope using geophysical, UAV, and geological techniques: Karakoram Himalaya, northern Pakistan. Front. Earth Sci. 9, 668011. https://doi.org/10.3389/feart.2021.668011

Khan AS, Hossain MM. 2001. Assessment of morphological changes due to construction of a barrage in the Teesta River. The 45th convention of IEB, Khulna, Bangladesh, 16–18 February 2001.

Kiedrzyńska E, Kiedrzyński M, Zalewski M. 2015. Sustainable floodplain management for flood prevention and water quality improvement. Nat. Hazards 76:955–977. https://doi.org/10.1007/s11069-014-1529-1

Kirby E, Whipple K. 2001. Quantifiying differential rock uplift rates via stream profile analysis. Geology 29(5):415–418. https://doi.org/10.1130/0091-7613(2001)029%3C0415:QDRURV%3E2.0.CO;2

Kraaijenbrink P, Meijer SW, Shea JM, Pellicciotti F, De Jong SM, Immerzeel WW. 2016. Seasonal surface velocities of a Himalayan glacier derived by automated correlation of unmanned aerial vehicle imagery. Ann. Glaciol. 57(71):103–113. https://doi.org/10.3189/2016AoG71A072

Langhammer J, Vacková T. 2018. Detection and mapping of the geomorphic effects of flooding using UAV photogrammetry. Pure Appl. Geophys. 175(9):3223–3245. https://doi.org/10.1007/s00024-018-1874-1

Le Heron DP, Vandyk TM, Kuang H, Liu Y, Chen X, Wang Y, Yang Z, Scharfenberg L, Davies B, Shields G. 2019. Bird's-eye view of an Ediacaran subglacial landscape. Geology 47(8):705–709. https://doi.org/10.1130/G46285.1

Li H, Zhao J, Yan B, Yue L, Wang L. 2022. Global DEMs vary from one to another: an evaluation of newly released Copernicus, NASA and AW3D30 DEM on selected terrains of China using ICESat-2 altimetry data. Int. J. Digit. Earth 15 (1):1149–1168. https://doi.org/10.1080/17538947.2022.2094002

Lukram IM, Tandon SK. 2022. Tributary fans of the Middle Teesta basin in Sikkim-Darjeeling Himalaya, NE India: their contribution to valley-filling processes. Geological Journal 57(2): 593–610. https://doi.org/10.1002/gj.4313

Mandal SP, Chakrabarty A. 2016. Flash flood risk assessment for upper Teesta river basin: using the hydrological modeling system (HEC-HMS) software. Model. Earth Syst. Environ. 2, 59. https://doi.org/10.1007/s40808-016-0110-1

Milan DJ, Heritage GL, Large AR, Fuller IC. 2011. Filtering spatial error from DEMs: implications for morphological change estimation. Geomorphology 125(1):160–171. https://doi.org/10.1016/j.geomorph.2010.09.012

Mirchandani M. 2016. The Teesta water dispute: geopolitics, myth and economics. Observer research foundation, India. https://policycommons.net/artifacts/1349535/the-teesta-water-dispute/1961694/ (accessed on 16 Jan 2024).

Mondal MSH, Islam MS. 2017. Chronological trends in maximum and minimum water flows of the Teesta River, Bangladesh, and its implications. Jamba: J. Disaster Risk Stud. 9(1), a373. https://doi.org/10.4102/jamba.v9i1.373

Mondal MS. 2022. Local scour at complex bridge piers in Bangladesh Rivers: reflections from a large study. Water 2022, 14, 2405. https://doi.org/10.3390/w14152405

Montgomery DR, Brandon MT. 2002. Topographic controls on erosion rates in tectonically active mountain ranges. Earth Planet. Sci. Lett. 201(3):481–489. https://doi.org/10.1016/S0012-821X(02)00725-2

Morris-Oswald T, Sinclair AJ. 2005. Values and floodplain management: case studies from the Red River Basin, Canada. Environ. Hazards 6(1):9–22. https://doi.org/10.1016/j.hazards.2004.10.001

Mullick RA, Babel MS, Perret SR. 2010. Flow characteristics and environmental flow requirements for the Teesta River, Bangladesh. In: Proceedings of International Conference on Environmental Aspects of Bangladesh (ICEAB10), Fukuoka, Japan, September 04, 2010, pp. 159–162.

NASA JPL, 2020. NASADEM Merged DEM Global 1 arc second V001 [Data set]. NASA EOSDIS Land Processes DAAC. https://doi.org/10.5067/MEaSUREs/NASADEM/NASADEM_HGT.001 (accessed on 11 May 2021)

Oguchi T, Hayakawa YS, Wasklewicz T. 2022. 6.50-Remote data in fluvial geomorphology: characteristics and applications. In: Shroder JF, (Eds.), Treatise on geomorphology (Second edition), Academic press, pp. 1116–1142. https://doi.org/10.1016/B978-0-12-818234-5.00103-6

Ogura T, Mizuno T, Katayama D, Yamanaka D, Sato Y. 2023. Estimating the amount of excavated soil using RTK-UAV in excavation projects that consider the habitat of rare species (in Japanese with English abstract). Ecol. Civil Eng. 22-00012. https://doi.org/10.3825/ece.22-00012

Özcan O, Özcan O. 2021. Multi-temporal UAV based repeat monitoring of rivers sensitive to flood. J. Maps. 17(3):163–170. https://doi.org/10.1080/17445647.2020.1820387

Palash W, Bajracharya SR, Shrestha AB, Wahid S, Hossain MS, Mogumder TK, Mazumder LC. 2023. Climate change impacts on the hydrology of the Brahmaputra River Basin. Climate 11, 18. https://doi.org/10.3390/cli11010018

Pangare G, Nishat B, Liao X, Qaddumi HM. 2021. The Restless River. World Bank, Washington, DC. https://doi.org/10.1596/36258 (accessed in March 2022).

Parizi E, Khojeh S, Hosseini SM, Moghadam YJ. 2022. Application of unmanned aerial vehicle DEM in flood modeling and comparison with global DEMs: case study of Atrak River Basin, Iran. J. Environ. Manage. 317, 115492. https://doi.org/10.1016/j.jenvman.2022.115492

Picco L, Pellegrini G, Iroumé A, Lenzi M, Rainato R. 2023. The role of in-channel vegetation in driving and controlling the geomorphic changes along a gravel-bed river. Geomorphology 437, 108803. https://doi.org/10.1016/j.geomorph.2023.108803

Piégay H, Kondolf GM, Minear JT, Vaudor L. 2015. Trends in publications in fluvial geomorphology over two decades: a truly new era in the discipline owing to recent technological revolution? Geomorphology 248:489–500. https://doi.org/10.1016/j.geomorph.2015.07.039

Prasai S, Surie MD. 2013. Political economy analysis of the Teesta River basin. The Asia Foundation, New Delhi. http://waterbeyondborders.net/wp-content/uploads/2017/06/TheAsiaFoundation.PoliticalEconomyAnalysisoftheTeestaRiverBasin.March20131.pdf (accessed in May 2022).

Raff JL, Goodbred SL, Pickering JL, Sincavage RS, Ayers JC, Hossain MS, Wilson CA, Paola C, Steckler MS, Mondal DR, Grimaud J, Grall CJ, Rogers KG, Ahmed KM, Akhter SH, Carlson BN, Chamberlain EL, Dejter M, Gilligan JM, Hale RP, Khan MR, Muktadir MG, Rahman MM, Williams LA. 2023. Sediment delivery to sustain the Ganges-Brahmaputra delta under climate change and anthropogenic impacts. Nat. Commun. 14, 2429. https://doi.org/10.1038/s41467-023-38057-9

Rahman MM, Arya DS, Goel NK, Dhamy AP. 2011. Design flow and stage computations in the Teesta River, Bangladesh, using frequency analysis and MIKE 11 modeling. J. Hydrol. Eng. 16:176–186. https://doi.org/10.1061/(ASCE)HE.1943-5584.0000299

Rai N, Neupane S, Rana S, Belbase D, Khawas V. 2019. Built on sand an examination of the practice of sand mining in south Asia with reflections from the Mahakali and the Teesta rivers. Policy Entrepreneurs Incorporated (PEI), Bakhundole, Lalitpur. Available at www.pei.center. https://pei.center/wp-content/uploads/2019/09/Policy-Brief-Built-on-Sand-20Sept2019-Final.pdf (accessed on Jan 2023).

Rajakumari S, Mahesh R, Sarunjith KJ, Ramesh R. 2022. Volumetric change analysis of the Cauvery delta topography using radar remote sensing. Egypt. J. Remote Sens. Space Sci. 25(3):687–695. https://doi.org/10.1016/j.ejrs.2022.06.003

Ramsankaran R, Navinkumar PJ, Dashora A, Kulkarni A. 2020. UAV-based survey of Glaciers in Himalayas: opportunities and challenges. J. Indian Soc. Remote Sens. 49:1171–1187. https://doi.org/10.1007/s12524-020-01300-7

Rhee DS, Kim YD, Kang B, Kim D. 2018. Applications of unmanned aerial vehicles in fluvial remote sensing: an overview of recent achievements. KSCE J. Civ. Eng. 22:588–602. https://doi.org/10.1007/s12205-017-1862-5

Rinaldi M, Belletti B, Bussettini M, Comiti F, Golfieri B, Lastoria B, Surian N. 2017. New tools for the hydromorphological assessment and monitoring of European streams. J. Environ. Manag. 202:363–378. https://doi.org/10.1016/j.jenvman.2016.11.036

Rumsby B, Brasington J, Langham J, McLelland S, Middleton R, Rollinson G. 2008. Monitoring and modelling particle and reach-scale morphological change in gravel-bed rivers: applications and challenges. Geomorphology 93:40–54. https://doi.org/10.1016/j.geomorph.2006.12.017

Rusnák M, Sládek J, Kidová A, Lehotský M. 2018. Template for high-resolution river landscape mapping using UAV technology. Measurement 115:139–151. https://doi.org/10.1016/j.measurement.2017.10.023

Saito H, Uchiyama S, Hayakawa YS, Obanawa H. 2018. Landslides triggered by an earthquake and heavy rainfalls at Aso volcano, Japan, detected by UAS and SfM-MVS photogrammetry. Prog. Earth Planet. Sci. 5, 15. https://doi.org/10.1186/s40645-018-0169-6

Salandra ML, Roseto R, Mele D, Dellino P, Capolongo D. 2022. Probabilistic hydro-geomorphological hazard assessment based on UAV-derived high-resolution topographic data: the case of Basento river (Southern Italy). Sci. Total Environ. 156736. https://doi.org/10.1016/j.scitotenv.2022.156736

Salmoral G, Rivas Casado M, Muthusamy M, Butler D, Menon PP, Leinster P. 2020. Guidelines for the use of unmanned aerial systems in flood emergency response. Water, 12(2), 521. https://doi.org/10.3390/w12020521

Sattar A. 2023. Sikkim glacial lake outburst spotlights climate vulnerability of the Himalayas. Nat. India. https://doi.org/10.1038/d44151-023-00152-7 (accessed on 16 Jan 2024).

Schwat E, Istanbulluoglu E, Horner-Devine A, Anderson S, Knuth F, Shean D. 2023. Multi-decadal erosion rates from glacierized watersheds on Mount Baker, Washington, USA, reveal topographic, climatic, and lithologic controls on sediment yields. Geomorphology 438, 108805. https://doi.org/10.1016/j.geomorph.2023.108805

Schwanghart W, Scherler D. 2017. Bumps in river profiles: uncertainty assessment and smoothing using quantile regression techniques. Earth Surf. Dyn. 5:821–839. https://doi.org/10.5194/esurf-5-821-2017

Şerban G, Rus I, Vele D, Breţcan P, Alexe M, Petrea D. 2016. Flood-prone area delimitation using UAV technology, in the areas hard-to-reach for classic aircrafts: case study in the north-east of Apuseni Mountains, Transylvania. Nat. Hazards 82(3):1817–1832. https://doi.org/10.1007/s11069-016-2266-4

Serra-Llobet A, Jähnig SC, Geist J, Kondolf GM, Damm C, Scholz M, Lund J, Opperman JJ, Yarnell SM, Pawley A, Shader E, Cain J, Zingraff-Hamed A, Grantham TE, Eisenstein W, Schmitt R. 2022. Restoring rivers and floodplains for habitat and flood risk reduction: experiences in multi-benefit floodplain management from California and Germany. Front. Environ. Sci. 9, 778568. https://doi.org/10.3389/fenvs.2021.778568

Sharma TPP, Zhang J, Koju UA, Zhang S, Bai Y, Suwal MK. 2019. Review of flood disaster studies in Nepal: a remote sensing perspective. Int. J. Disaster Risk Reduct. 34:18–27. https://doi.org/10.1016/j.ijdrr.2018.11.022

Simon A, Rinaldi M. 2006. Disturbance, stream incision, and channel evolution: the roles of excess transport capacity and boundary materials in controlling channel response. Geomorphology 79(3-4):361–383. https://doi.org/10.1016/j.geomorph.2006.06.037

Śledź S, Ewertowski M, Piekarczyk J. 2021. Applications of Unmanned Aerial Vehicle (UAV) surveys and structure from motion photogrammetry in glacial and periglacial geomorphology. Geomorphology 378, 107620.

Smith MW, Carrivick JL, Quincey DJ. 2015. Structure from motion photogrammetry in physical geography. Progr. Phys. Geogr. 40:1–29. https://doi.org/10.1177/0309133315615805

Stott T. 2013. Review of research in fluvial geomorphology 2010–2011. Prog. Phys. Geogr. 37(2):248–258. https://doi.org/10.1177/0309133313477124

Sultana MR. 2022a. Bank Erosion and sediment deposition in Teesta River: A spatiotemporal analysis. In: Bhunia GS, Chatterjee U, Lalmalsawmzauva K, Shit PK. (Eds.), Anthropogeomorphology. Geography of the physical environment. Springer, Cham, pp. 73–89. https://doi.org/10.1007/978-3-030-77572-8_4

Sultana MR. 2022b. Dislocation and involuntary migration: lessons from the Teesta River bank erosion in Bangladesh. In: Mishra M, Singh RB, Lucena AJd, Chatterjee S. (Eds.), Regional development planning and practice. advances in geographical and environmental sciences. Springer, Singapore, pp. 121–147. https://doi.org/10.1007/978-981-16-5681-1_6

Syed A, Haq A, Uzzaman A, Goodrich CG, Mallick D, Mini G, Sharma G, Nyima K, Mamnun N, Varma N, Singh P, Ghate R, Triwedi S, Sen S, Bhadwal S, Hassan T, Dilshad T, Gulati V, Naznin Z. 2017. The Teesta basin: enough water for power and agriculture for all?. Himalayan adaptation, water and resilience (HI-AWARE) working paper 12, Nepal. https://lib.icimod.org/record/33669 (accessed on 18 Jan 2024).

Tang C, Tanyas H, Van Westen CJ, Tang C, Fan X, Jetten VG. 2019. Analysing post-earthquake mass movement volume dynamics with multi-source DEMs. Eng. Geol. 248:89–101. https://doi.org/10.1016/j.enggeo.2018.11.010

Tarannum T, Bhuyan A, Badhon FF. 2018. Morphological changes of river Teesta during the Last decade. In: Proceedings of the 1st national conference on water resources engineering (NCWRE-2018), CUET, Chittagong, Bangladesh, 21-22 March 2018.

Tempa K, Peljor K, Wangdi S, Ghalley R, Jamtsho K, Ghalley S, Pradhan P. 2021. UAV technique to localize landslide susceptibility and mitigation proposal: a case of Rinchending Goenpa landslide in Bhutan. Nat. Hazards Res. 1(4):171–186. https://doi.org/10.1016/j.nhres.2021.09.001

Tran T, Nguyen BQ, Vo ND, Le M, Nguyen Q, Lakshmi V, Bolten JD. 2023. Quantification of global Digital Elevation Model (DEM)–a case study of the newly released NASADEM for a river basin in Central Vietnam. J. Hydrol.: Regional Studies 45, 101282. https://doi.org/10.1016/j.ejrh.2022.101282

Tseng CM, Lin CW, Stark CP, Liu JK, Fei LY, Hsieh YC. 2013. Application of a multi-temporal, LiDAR-derived, digital terrain model in a landslide-volume estimation. Earth Surf. Process Landf. 38:1587–1601. https://doi.org/10.1002/esp.3454

Tsunetaka H, Hotta N, Hayakawa YS, Imaizumi F. 2020. Spatial accuracy assessment of unmanned aerial vehicle-based structures from motion multi-view stereo photogrammetry for geomorphic observations in initiation zones of debris flows, Ohya landslide, Japan. Prog Earth Planet Sci. 7(1):1–14. https://doi.org/10.1186/s40645-020-00336-0

Uuemaa E, Ahi S, Montibeller B, Muru M, Kmoch A. 2020. Vertical accuracy of freely available global digital elevation models (ASTER, AW3D30, MERIT, TanDEM-X, SRTM, and NASADEM). Remote Sens. 12(21), 3482. https://doi.org/10.3390/rs12213482

Van Denderen RP, Kater E, Jans LH, Schielen RMJ. 2022. Disentangling changes in the river bed profile: the morphological impact of river interventions in a managed river. Geomorphology 408, 108244. https://doi.org/10.1016/j.geomorph.2022.108244

Van Iersel WK, Addink EA, Straatsma MW, Middelkoop H. 2016. River floodplain vegetation classification using multi-temporal high-resolution colour infrared UAV imagery. In proceedings of the GEOBIA 2016: solutions and synergies, Enschede, The Netherlands, 14–16 September 2016.

Van Woerkom T, Steiner JF, Kraaijenbrink PDA, Miles ES, Immerzeel WW. 2019. Sediment supply from lateral moraines to a debris-covered glacier in the Himalaya. Earth Surf. Dynam. 7:411–427. https://doi.org/10.5194/esurf-7-411-2019

Wang S, Ren Z, Wu C, Lei Q, Gong W, Ou Q, Zhang H, Ren G, Li C. 2019. DEM generation from Worldview-2 stereo imagery and vertical accuracy assessment for its application in active tectonics. Geomorphology 336:107–118. https://doi.org/10.1016/j.geomorph.2019.03.016

Wang T, Watanabe T. 2022. Monitoring campsite soil erosion by structure-from-motion photogrammetry: a case study of Kuro-dake Campsites in Daisetsuzan national park, Japan. J. Environ. Manage. 314, 115106. https://doi.org/10.1016/j.jenvman.2022.115106

Watson CS, Kargel JS, Tiruwa B. 2019. UAV-Derived Himalayan topography: hazard assessments and comparison with global DEM products. Drones 3(1), 18. https://doi.org/10.3390/drones3010018

Wobus C, Whipple KX, Kirby E, Synder N, Johnson J, Spyropolon K, Crosby B, Sheehan D. 2006. Tectonics from topography: Procedures, promise, and pitfalls. In: Willett SD, Hovius N, Brandon MT, Fisher DM. (Eds.), Tectonics, climate, and landscape evolution. Geol. Soc. Am. Special paper 398, pp. 55–73. https://doi.org/10.1130/2006.2398(04)

Woodget AS, Carbonneau PE, Visser F, Maddock IP. 2014. Quantifying submerged fluvial topography using hyperspatial resolution UAS imagery and structure from motion photogrammetry. Earth Surf. Process Landf. 40:47– 64. https://doi.org/10.1002/esp.3613

Wohl E. 2014. Time and the rivers flowing: fluvial geomorphology since 1960. Geomorphology 216(1):263–282. https://doi.org/10.1016/j.geomorph.2014.04.012

Wheaton JM, Brasington J, Darby SE, Sear DA. 2010. Accounting for uncertainty in DEMs from repeat topographic surveys: improved sediment budgets. Earth Surf. Process Landf. 35:136–156. https://doi.org/10.1002/esp.1886

Yang C, Jen C, Cheng Y, Lin J. 2021. Quantification of mudcracks-driven erosion using terrestrial laser scanning in laboratory runoff experiment. Geomorphology 375, 107527. https://doi.org/10.1016/j.geomorph.2020.107527

Zarfl C, Lumsdon AE, Berlekamp J, Tydecks L, Tockner k. 2015. A global boom in hydropower dam construction. Aquat. Sci. 77:161–170. https://doi.org/10.1007/s00027-014-0377-0